MARMARA UNIVERSITY
INSTITUTE FOR GRADUATE STUDIES
IN PURE AND APPLIED SCIENCES

SIMPLIFIED MULTIBODY SYSTEM DYNAMICS MODELING AND PERFORMANCE EVALUATION OF ELECTRICAL LOCOMOTIVES

ŞAFAK ALKAN

MASTER THESIS

Department of Mechanical Engineering

ADVISOR

Prof. Dr. A. Kerim KAR

ISTANBUL, 2013

MARMARA UNIVERSITY
INSTITUTE FOR GRADUATE STUDIES
IN PURE AND APPLIED SCIENCES

SIMPLIFIED MULTIBODY SYSTEM DYNAMICS MODELING AND PERFORMANCE EVALUATION OF ELECTRICAL LOCOMOTIVES

ŞAFAK ALKAN

MASTER THESIS

Department of Mechanical Engineering

ADVISOR

Prof. Dr. A. Kerim KAR

ISTANBUL, 2013

ACKNOWLEDGEMENT

First of all, I would like to thank my supervisor Prof.Dr. Abdülkerim Kar and project coordinator Prof.Dr. Erturul Taçgın, for the valuable guidance and advice on preparing this thesis and giving me moral and material support. I would also like to thank Haydar Şahin who studied in the project and supplied us to get complimentary support from İstanbul Ulaşım A.Ş.

I would also like to thank The Scientific and Technological Research Council of Turkey (TÜBİTAK), for giving our group the chance of working on this project.

Finally, I would like to acknowledge my research assistant friends who we work together in the same office in the engineering faculty. Also, I want to say thank you to my family for their complimentary support.

June, 2013 Şafak ALKAN

TABLE OF CONTENTS

ÖZET

Elektrikli Lokomotiflerin Basitleştirilmiş Çoklu Gövdeli Sistemler Yoluyla Dinamik Modellenmesi ve Performanslarının Değerlendirilmesi

Lokomotiflerin dinamik modellemesi ve simulasyonları, raylı taşıtların enerji verimliliği, güvenliği ve yolcu rahatlığı açısından optimal tasarımda önemli rol oynar. Günümüzde, çoklu gövdeli sistem dinamik modellemeleri ve çeşitli programlar kullanılarak yapılan simulasyonlar genellikle bu amaç için kullanılmaktadır.

Türkiye'de son yıllarda demiryolu taşımacılığı önemli ölçüde gelişme kaydetmektedir. Ancak Türkiye'de çoklu gövdeli sistem dinamiği konusunda yeterli çalışma yapılmamaktadır. Bu çalışmada sistem dinamiği yöntemi kullanılarak, ADAMS/Rail programında bir dinamik simulasyon modeli oluşturulmuştur. Çoklu gövdeli model referans alınan Universal Mechanism (yazılım geliştirme grubu) modeline benzer bir şekilde tasarlanmıştır. Oluşturulan modelin dinamik davranışları, TÜBİTAK'ın Tren Simulasyou Projesindeki gerçek verilerle karşılaştırılmış ve başarı oranı değerlendirilmiştir.

İlk olarak ADAMS/Rail yazılımında, tekerlek seti, boji ve yaklaşık 70 serbestlik derecesine sahip olan tüm lokomotif sisteminin modellemesi ve analizi gerçekleştirilmiştir. TRENSIM projesinden alınan gerçek salınım verileriyle karşılaştırılıp, önceden belirlenmiş standartlara uygun olarak bu çalışmaya en uygun yol düzensizliği belirlenmiştir. Kararlılık ve dinamik analizlerinin bir sonucu olarak, modelin kritik hızları ve doğal frekansları hesaplanmıştır. Ayrıca, öz değerler ve öz vektörler hesaplanıp sistemin kararlı olup olmadığı test edilmiştir.

Haziran, 2013 Şafak ALKAN

ABSTRACT

Simplified Multibody System Dynamics Modeling and Performance Evaluation of Electrical Locomotives

Dynamic modeling and simulation of locomotives are very important for the optimal design of the railroad vehicles for safety, comfort and efficiency. Nowadays, multibody system dynamics modeling and computer simulation using various programs have been utilized usually for this purpose.

In recent years, the railway transportation has been considerably developed in Turkey. Hovewer, Turkey does not have sufficient research about multibody dynamics. In this study, a dynamic simulation model has been built in ADAMS/Rail program using the multibody system dynamics methodology. Multibody dynamic model has been created similar to the Universal Mechanism (developed by group of software laboratory) model. The dynamic behavior of the models have been compared with the real data in Train Simulator Project of TUBITAK and success rate has been assessed.

Firstly, the wheelset, bogie and whole locomotive which has about 70 degrees of freedom have been modeled and analyzed in ADAMS/Rail. By comparing the oscillation values with the real data, the optimal type of track irregularity has been approved for this study with respect to the predefined standards. As a result of the stability and dynamic analysis, the critical speeds and natural frequencies of the models have been determined. Also, the eigen vectors and eigen values have been determined to test whether the systems are stable.

June, 2013 Şafak ALKAN

SYMBOLS

A	**:** The roughness constant
$\boldsymbol{c(\sqrt{ab})}$	**:** The contact elipse between wheel and rail
$\mathbf{c_h}$	**:** A constant related to properties of material and radius [Nm-3/2]
$\mathbf{c_{ij}}$	**:** Stiffness coefficient
$\mathbf{F_c}$	**:** The centrifugal component of the force (N)
$\mathbf{F_0}$	**:** The magnitude of friction force (N)
$\boldsymbol{M}$	**:** Total number of harmonics
$\mathbf{S_c(\omega)}$	**:** The PSD function (m^2/(rad/m))
$\mathbf{S_{zz}}$	**:** Power spectral density (m^2/m^{-1})
$\boldsymbol{\dot{z}}$	**:** The relative velocity of motion (m/s)
$\boldsymbol{\lvert\dot{z}\rvert}$	**:** The magnitude of velocity ($m.s^{-1}$)
$\mathbf{\Delta s}$	**:** The irregularity step size
$\mathbf{\Delta\omega}$	**:** The frequency increment (rad/m)
$\boldsymbol{\varphi(m\Delta\omega)}$	**:** The phase uniformly distributed on interval $[-\pi, \pi]$
γ_{eq}	**:** The equivalent conicity
$\boldsymbol{\xi}$	**:** Creepage of wheels
$\boldsymbol{\mu}$	**:** Friction coefficient
$\mathbf{\Lambda}$	**:** Wavelength (m)
$\boldsymbol{\lambda}$	**:** Conicity
$\emptyset$	**:** Spatial frequency (m^{-1})
$\emptyset_1, \emptyset_2$	**:** Cutoff spatial frequencies (m^{-1})

ABBREVIATIONS

CM	**:** Center of Mass
FRA	**:** Federal Railway Administration
LOCO	**:** Locomotive
PSD	**:** Power Spectrum Density
TRENSIM	**:** Train Simulator Project of TÜBİTAK
TÜBİTAK	**:** The Scientific and Technological Research Council of Turkey
UM	**:** Universal Mechanism
WEB	**:** Wheelset Electromotor Block

LIST OF FIGURES

LIST OF TABLES

1. INTRODUCTION

Rail vehicle dynamics is one of the important engineering research area. Modern vehicles have been developed through research and experiments. With the recent development of computer software, it is possible to acquire extensive knowledge about the behavior of the vehicles. Information about the forces coming from rails are determined according to the rail quality standards. These standards have been developed to calculate the critical speed all over the world. Although these standards and multibody locomotive dynamic software are available abroad, it is not available in our country.

Rail transport system plays a significant role for the transport of passengers and goods. The production of high-speed trains is increasing everyday all over the world, and especially in Turkey. Accordingly, the work done on vehicle dynamics has a great importance because of the increasing passenger loads, tight curves, and increasing speeds. For this reason, Turkey is obliged to develop her own programs for real-time behaviour of rail vehicles.

1.1. Objectives of the Thesis

In fast moving transportation industry, Turkey also have studies on high-speed trains and rails today. There are some studies about mathematical modeling and simulators in Turkey. However, the modeling is an important requirement to run the simulations with using several dynamic equations for training the machinists. Our country does not have the required models. In the thesis, a locomotive model will be set up in ADAMS/Rail software within the scope of TUBITAK Project. The main aim of this thesis is to set up the model and to compare the simulation results with the measured data from TRENSIM Project. Therefore, the success rate will be assessed. This study will shape the commercial success in this direction and important steps will be taken for the future.

1.2. Literature Review

In this section, the domestic and foreign literature studies and the general information have been presented about the thesis.

1.2.1. Track irregularity research

The distributed irregularity of the track is described by means of its PSD (power spectrum density), S_{zz}, expressed in terms of the spatial frequency $\emptyset$ (number of cycles per unit of length). The corresponding PSD, $\bar{S}_{zz,}$ in the frequency domain is easily deduced as [1]

$$\bar{S}_{zz}(f) = \frac{S_{zz}(\emptyset)}{v_0} \tag{1.1}$$

where v_0 is the speed of the vehicle.

From various representations found in the literature, the functions proposed by Garg and Dukkipati [2] were retained because they present a wide classification (6 classes—from good to very bad quality) and are based on the large data collected in the U.S. by the Federal Railway Administration (FRA). As the vertical motion is considered in the simulation and a 2D model is derived for the track, only the vertical profile is taken into account, and the cross level is neglected. The gauge and the lateral alignment do not intervene. The vertical profile PSD is then expressed in the following way

$$S_{zz}(\emptyset) = \frac{A\emptyset_2{}^2(\emptyset^2+\emptyset_1{}^2)}{\emptyset^4(\emptyset^2+\emptyset_1{}^2)} \tag{1.2}$$

with A the roughness constant and $\emptyset_1$ and $\emptyset_2$ two cutoff spatial frequencies. The evolution of the PSD of the vertical profile vs spatial frequency is presented in figure 1.2.1 for quality classes 1 to 6. According to Garg and Dukkipati, this representation should be limited to a wavelength range from 1.5 m to 300 m.

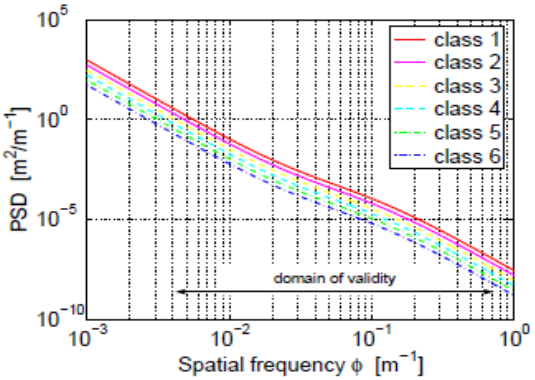

Figure 1.2.1. Power spectral density [1]

1.2.2. Wheel-rail contact research

In vehicle dynamics, the movement of bodies which have multi-degree of freedom increases the complexity of the system. When the structure of the wheel and rail contact is added on this, it becomes more complex. The first studies on this is based on the beginning of the 17th century. According to studies, higher speeds have been achieved with using flanged wheels to provide the necessary guidance. However, the occurring dynamic loads have continued to be a problem. Particularly, this effect was seen more frequently in the growing steam locomotives and breaks have occurred in rails. With the increase of speed, comfort has decreased and lateral oscillation problem has emerged. Scientific approach to the problem has been required by increasing of accident risks, and engineering approaches have increased by developing of software and hardware technology.

It is achieved easier rotation in curves with reducing the flange contact and conicity. Despite the positive effect of conicity in curves, it causes lateral displacements in a straight line.

In 1883, Klingel [3] revealed mathematical data about the lateral oscillation. Klingel stated the wavelength (Λ) with conicity (λ), radius (r_o) and the distance between the contact points (l).

$$\Lambda = 2\pi(r_o l/\lambda)^{1/2} \qquad (1.3)$$

Klingel's formula shows that as the speed is increased, so will the frequency of the kinematic oscillation. Figure 1.2.2 shows the kinematic oscillation of a wheelset.

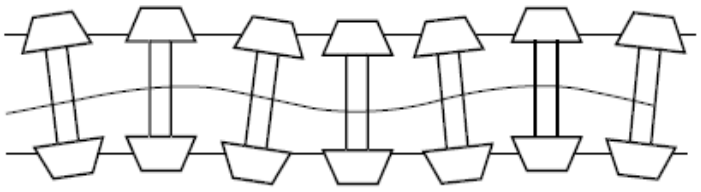

Figure 1.2.2. The kinematic oscillation of a wheelset

The action of a wheelset with coned wheels in a curve was understood intuitively early in the development of the railways. In 1829 Ross Winans [4] took out a patent that

stressed the importance of the axles taking up a radial position on curves. Adams [5] determined the limits of conicity that should be in curves and Redtenbacher [6] realized the first theoretical analysis of the movement of the wheel in curves.

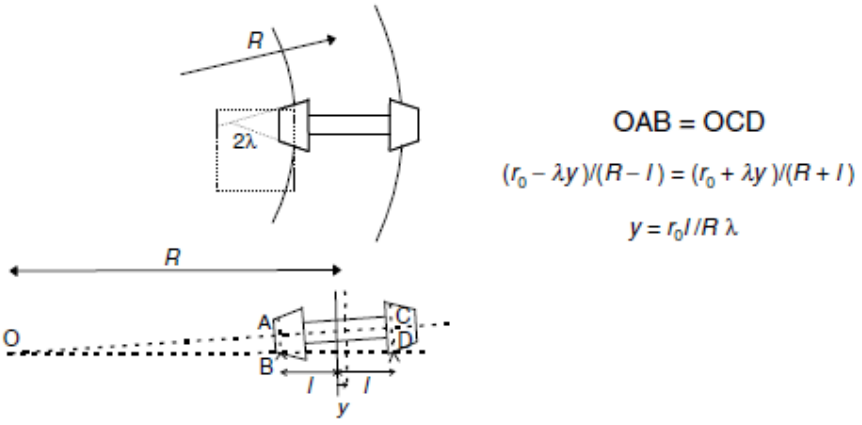

Figure 1.2.3. Rolling of a coned wheelset on a curve [6]

Creep, adhesion and wear have a three-way relationship. The geometry of the wheel and rail profiles affects the creep characteristics and they in turn influence the dynamic behavior of the vehicle. The effect of creep exists when two rigid bodies are in contact against each other with force and allowed to roll over each other. This contact region was first formed in Hertz's static theory [7].

In general, the circumferential velocities of the rolling bodies are not equal. A dimensionless term creepage is used to define these deviations from a pure rolling motion of the two bodies. Carter [8] was the first to recognize the significance of creep for applications in the dynamics of rail vehicles. Creeapage is defined in both the longitudinal (ξ_x) and lateral directions (ξ_y).

$$\xi x = \frac{\text{actual forward velocity} - \text{pure rolling forward velocity}}{\text{pure rolling forward velocity}} \qquad (1.4)$$

$$\xi y = \frac{\text{actual lateral velocity} - \text{pure rolling lateral velocity}}{\text{pure rolling forward velocity}} \qquad (1.5)$$

The tangential forces (creep forces) exerted between the wheel and rail play a major role in rail vehicle dynamics. They arise out of the difference in strain rates of the two

bodies in the contact region. Figure 1.2.4 shows the functional relationship between creepages, the creep forces and moments.

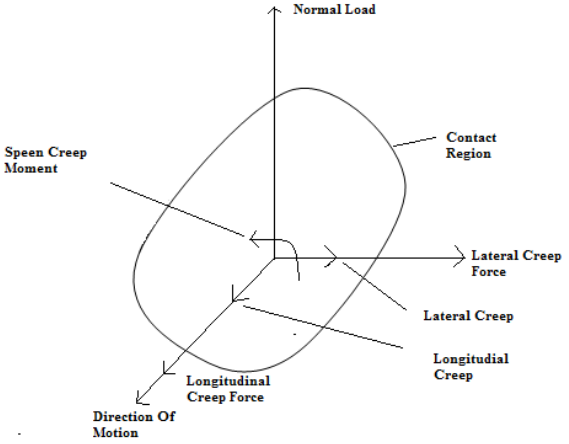

Figure 1.2.4. Creep, creep forces and creep moments

VL Markine and IY Shevtsov [9] investigated the wheel profile optimization on the basis of the exchange of the rolling radius, which account for the reduction of wear and contact stresses as well as for stability of the vehicle. The described procedure has been applied to improve the wheel profile design for a passenger train that was suffering from rolling contact fatigue defects in the rails and wheels. The failure criterion was formulated using the vehicle stability requirement with the Monte Carlo method. IY Shevtsov [10] also investigated the geometric contact between wheel and rail. Next, railway vehicle dynamics had been considered with the help of ADAMS/Rail multi-body dynamic simulation software. Finally a numerical optimization method had been used for the design of the wheel profile. The model of Shevtsov in ADAMS / Rail is seen in Figure 1.2.5.

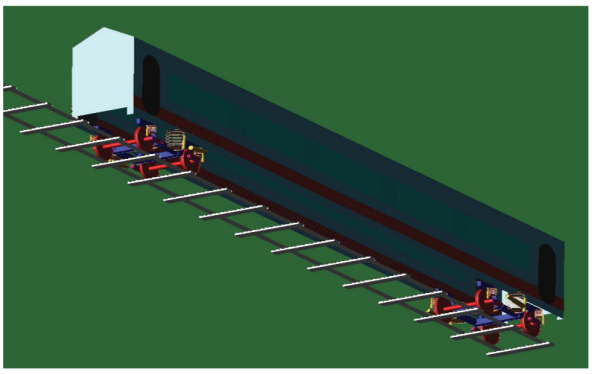

Figure 1.2.5. Complete railway system modelled in ADAMS / Rail [10]

M.M. Jalili and H. Salehi [11] applied progressive concept of correspondence to create new wheel/rail model based on the virtual penetration theory. The geometry and mechanism of contact have been solved simultaneously because of the independency in a defined correspondence. This model took the penetrated profiles of wheel and rail and also associated creeps as its inputs, and produces driving contact forces as its outputs.

Shen, Ayasse, Chollet and Pratt [12] developed a target-oriented method for the design of railway wheel profiles. The design methodology made use of a unique inverse method. This employed contact angles and rail profile information. A computer program based on this method has also been built and was validated by way of an example. This is an example of an implementation for an independent wheelset. The contact angles and comparision of create and original profile are shown below.

J. Evans and S.D. Iwnicki [13], specified that technical and economic problems occur when using inappropriate wheel profiles in lines. They also investigated the effect of conicity to wear. The pattern of wear varies enormously from application to application. Poor curving vehicles on curvaceous routes will suffer mainly flange wear, whereas good curving vehicles on relatively straight routes will suffer mainly tread wear.

At the larger curve radius, 1200 m to 1800 m, where rolling contact fatique is most prevalent, it will be seen that the contact stress drops as the wear increases. At tighter radius the contact stresses can start to rise quite rapidly, but these curves are less inclined to rolling contact fatique.

1.2.3. Railway Vehicle Model Research

Rail transport system plays a significant role for the transport of passengers and goods. In fast moving transportation industry, the production of high-speed trains is increasing everyday all over the world. There has been many researches about this topic.

Dmitry Agapov [14] described a simplified and full model of loco E43000 which consists of many nonlinear elements, closed kinematical loops, wheelset subsystems, bogies subsystems and a main system. Most of bodies in models were imported in UM format from Solidworks models created by drawings, documentation and photos that were provided by Marmara Research Center. The rest of bodies are created in UM from

standard primitives. At the end of the report some simulation results were presented. The hierarchy of subsystems are shown in figure 1.2.6.

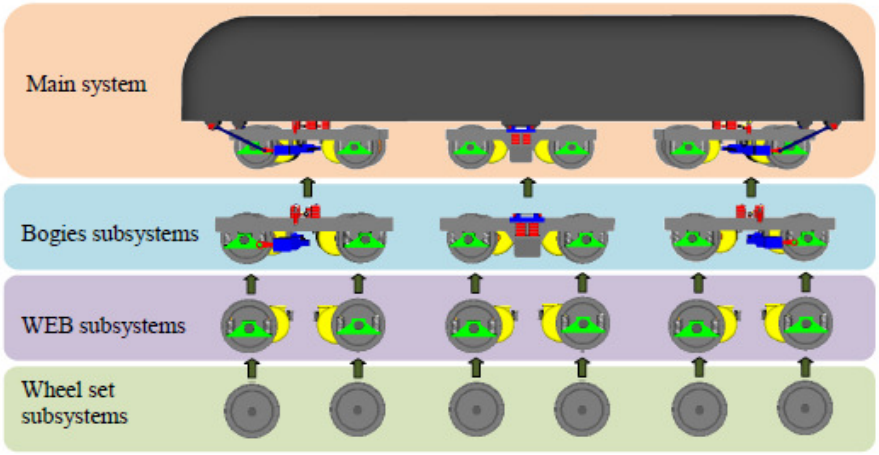

Figure 1.2.6. Subsytems hierarchy [14]

Brian James Sperry [15] investigated the dynamic behavior of the truck under warping conditions using a stand-alone model created in Virtual Lab. The model with extremely worn sideframes allowed for investigation into the effects of wear on the damping abilities and warp stiffness of the truck.

Fujie, Jian, Lijian and Quanbao [16] modified the dynamic performance of electric locomotive SS7CG. The model was analyzed and simulated using ADAMS/Rail. The critical speed for non-linear stability on curved track, dynamic performance negotiation on various curved tracks, comfort study and axle load transference were calculated. The dynamic performance of the modified Locomotive SS7CG could completely meet the requirement of running speed of 160 km/h.

Müller, Kögel and Schreiber [17] simulated the mechanical behaviour of a railway vehicle. Here, ADAMS/Rail model has been developed which describes the structural dynamical behaviour and the contact between wheel and rail in more detail. The control part created by MATLAB/SIMULINK and the mechanical part created by ADAMS/Rail were coupled and this mechatronical simulation model was used for a more reliable control unit design.

Michalek and Zelenka [18] dealed with influence of nose-suspended traction drive of a locomotive on the dynamic interaction between the vehicle and the track. By means of

simulations, dynamic behaviour of the locomotive with axle-mounted traction motors was compared with dynamic behaviour of a locomotive equipped with fully suspended traction drive. The nose-suspended traction motor in this study is shown in figure 1.2.7.

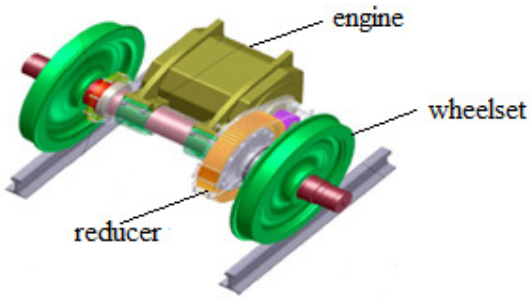

Figure 1.2.7. Nose-suspended traction motor [18]

Robert F. Harder [19] developed a load-dependent friction wedge model using the ADAMS / View environment. After this model was validated against theoretical benchmarks, it was imported into an ADAMS/ Rail vehicle model of a typical North American three-piece bogie. The results of model development for both the friction wedge and three-piece bogie has been presented, as well as ADAMS/Rail simulation results of the bogie dynamics under a variety of operating conditions.

Gugliotta and Soma [20] studied the stability analysis and high speed transient simulation of a railway vehicle using ADAMS/ Rail. The dynamic of a railway vehicle was studied including different wheel-rail contact models in order to evaluate the critical speed with reference to Kalker's contact theory [21].

Sen-Yung Lee and Yung-Chang Cheng [22] proposed a new dynamic model of railway vehicle moving on curved tracks. In the new model, the motion of the car body was considered and the motion of the truck frame was not restricted by a virtual boundary. Based on the heuristic nonlinear creep model, the nonlinear coupled differential equations of the motion of an eight degrees of freedom car system considering the lateral displacement and the yaw angle of each wheelset.

Brent S. Ballew [23] created a half-truck model which comprised of four rigid bodies: a bolster, two friction wedges, and a sideframe assembly. The model allowed each wedge four degrees of freedom: vertical displacement, longitudinal displacement (between the

bolster and sideframe), pitch (rotation around the lateral axis), and yaw (rotation around the vertical axis).

Zboinski and Dusza [24] aimed to study at more accurate stability analysis of railway vehicles in a curved track and studied on nonlinear critical velocity and the linear system critical velocity shown in figure 1.2.8.

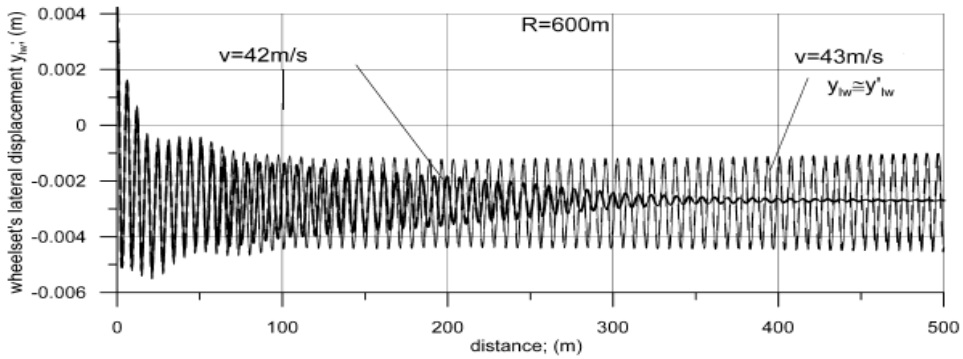

Figure 1.2.8. The lateral displacement and critical speed of wheelset [24]

Uzzal, Ahmed and Rakheja [25] presented the responses of the railway vehicle and track components in terms of contact forces and displacements. The considered vehicle model has five-DOF. The car body was linked with the vehicle bogie through secondary suspension springs and damper elements, which was further linked to the wheels through primary suspension springs and damper elements.

Parena, Kuka, Vivalda and Kik [26] aimed to obtain a good curving performance, ride quality and a high passenger comfort and to reduce the noise level. They made the theoretical analysis of vehicle with help of ADAMS/Rail - MEDYNA modeling and simulations.

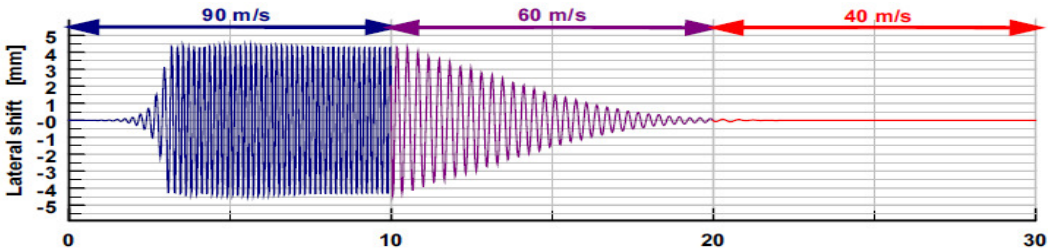

Figure 1.2.9. The lateral shift of model in ADAMS/Rail – MEDYNA [26]

A. Shabana, H. Zaher, M. Recuero and Rathod [27] examined the stability of linear systems using an eigenvalue analysis that employes constant eigenvalues and eigenvectors. For the linear system, the mass, stifness and damping matrices were constant and independent of time and system configuration. The nonlinear equations of motion of the gyroscope were formulated using two different sets of orientation parameters.

1.3. Scope of the Thesis

The main objective of this thesis is to develop a multibody dynamic model which is similar to the Universal Mechanism model developed by group of software laboratory and, to compare the simulation results and the dynamic behavior of the model with the real data in Train Simulator Project of TUBITAK. The importance of the work can be illustrated in the demonstration of railway system application modeling and make the necessary analysis for the studied system to study the dynamic behavior of the railway vehicle.

The work proposed here has been presented in four chapters. In Chapter 1, the description of the problem has been mentioned and the studies made about this subject have been investigated. Chapter 2 provides the description and methodology of materials and models clearly. The track model and track irregularity used in the dynamic simulation of models on the straight and curved ways have been presented. Also, the importance of wheel-rail contact has been adverted. The modeling of wheelset, bogie and locomotive have been explained. Chapter 3 includes the stability and dynamic analysis results of single wheelset, bogie and locomotive models which occured in ADAMS/Rail. The kinematic and dynamic behaviour of the models have been demonstrated and compared with the real data of TRENSIM Project. The obtained results have been discussed fort he studied model. Finally, in Chapter 4, the overall conclusions and perspectives have been described.

2. MATERIAL AND METHOD

In this section, the materials used and the methods have been clearly described. The track irregularity model, the wheel-rail contact part and the modeling of the locomotive and its parts have been presented respectively.

2.1. Track Modeling

In this part, the specification of the track used in the dynamic simulation on a curve has been represented. The track reference frame represented by the three orthogonal axes (X_T, Y_T, Z_T) which assign to the centerline between the left rail and right rail as shown in figure 2.1.1, where X_T, Y_T and Z_T axes are pointing to the longitudinal, lateral and vertical direction of the railway vehicle.

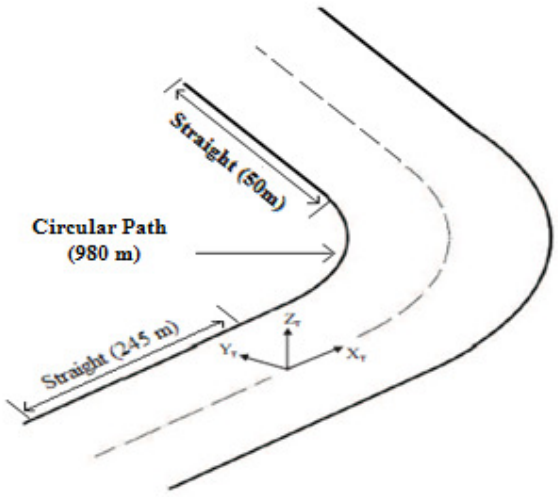

Figure 2.1.1. Track model used in the dynamic simulation o a curve

The track starts with a straight segment and continues along 245 meters as shown. After that, the track takes a circular path with a linearly increased radius of curvature between 0-300 m and continues along 245 meters. Then, the track continues along 490 meters on a circular path with a constant radius of curvature R (300 m). The track again continues with a 245 meters linearly decreased circular path. Finally, the track finishes with a 50 meters straight segment and dynamic simulation stops. Here, the track has no irregularities.

When traveling in horizontal curves, railway vehicles are influenced by centrifugal forces, which act in a direction a way from the center of the curve to over turn the vehicle. The sum of a vehicle weight and its centrifugal forces produced a resultant force directed to the outer rail. In order to counteract this force, the outer rail in a curve is raised. The difference in hight between the outer and the inner rail plane is called the cant or the super elevation h_t, which can be defined as shown in figure 2.1.2.

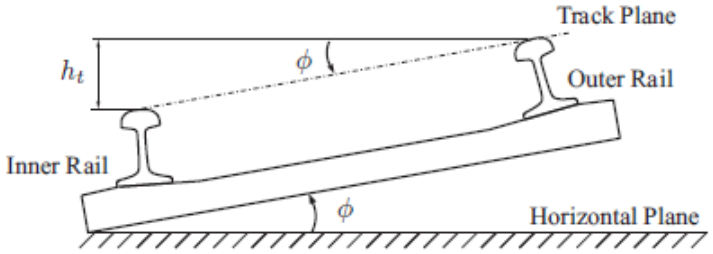

Figure 2.1.2. Cant and cant angle

2.2. Track Irregularity

Track irregularities can be generated according to specified PSD (power spectrum density) function. The algorithm is used to generate the irregularity functions according to the formula [14] :

$$x[n\Delta s] = \sum_{m=0}^{M} \sqrt{2S_c(m\Delta\omega)\Delta\omega}\, cos[m\Delta\omega n\Delta s + \varphi(m\Delta\omega)] \qquad (2.1)$$

where Δs is the irregularity step size, m; M is the total number of harmonics in the sum; $S_c(\omega)$ is the PSD function, m^2/(rad/m); Δω is the frequency increment, rad/m; $\varphi(m\Delta\omega)$ is the phase uniformly distributed on interval $[-\pi, \pi]$. The PSD can be function of frequency measured both in rad/m (circular frequency) and in cycles/m.

The power spectrum density has been converted to irregularity in terms of distance and phase angle with using Fourier series in MATLAB. These studies have been made for six types of track irregularities in ABD Standards [1].

When comparing the vertical displacement of wheelset in TRENSIM project (Figure 2.2.1), the second type of track irregularity has been approved for this study as seen in figure 2.2.2. The other types are shown in APPENDIX B.

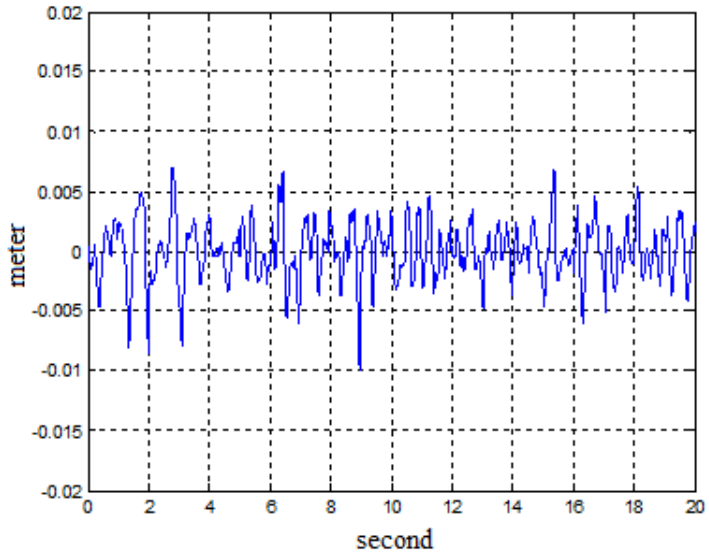

Figure 2.2.1. Vertical displacement of wheelset (TRENSIM Project)

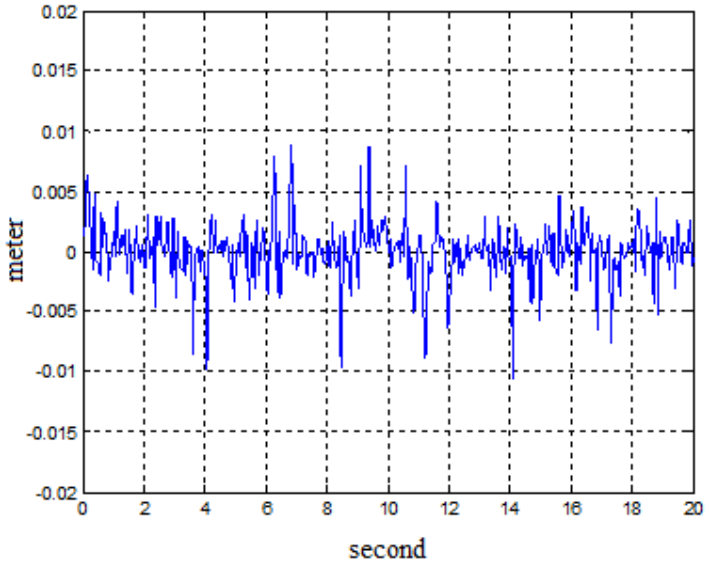

Figure 2.2.2. Second type of track irregularity [1]

Then the parameters which belong to second type of track irregularity in UM Model, have been used in ADAMS/Rail and a random track irregularity has been occured as seen in figure 2.2.3. These parameters are shown in table 2.2.1.

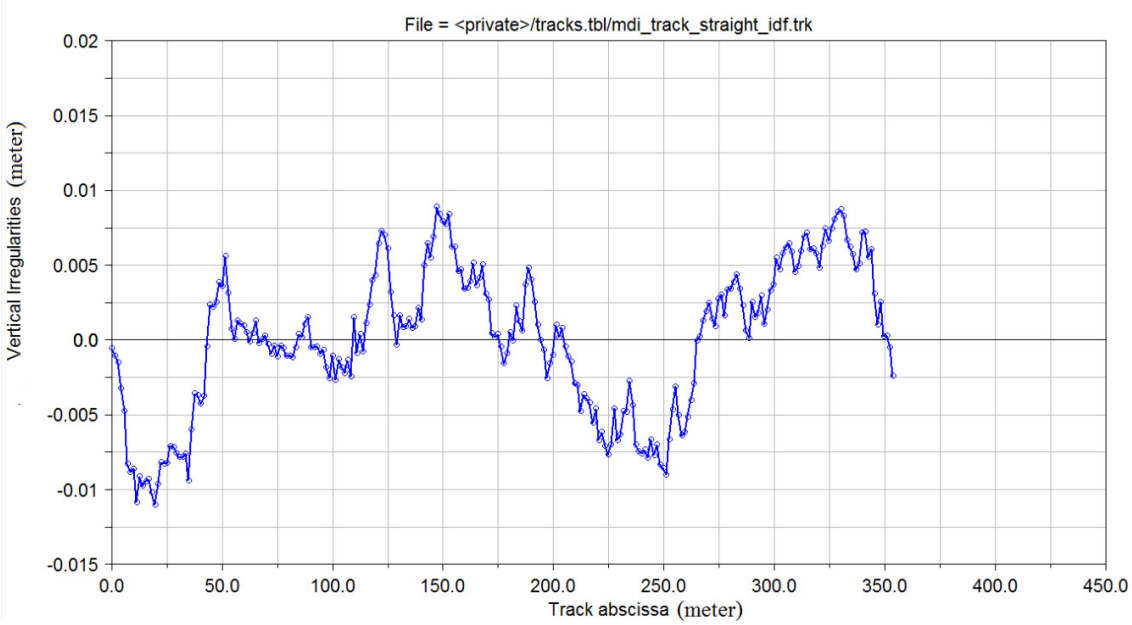

Figure 2.2.3. Second type of track irregularity in ADAMS/Rail

Table 2.2.1. The parameters of track irregularity [14]

Class	Parameter			
	A_v, cm^2 rad/m	A_a, cm^2 rad/m	Ω_s, rad/m	Ω_c, rad/m
1 (worst)	1,2107	3,3634	0,6046	0,8245
2	1,0181	1,2107	0,9308	0,8245
3	0,6816	0,4128	0,8520	0,8245
4	0,5376	0,3027	1,1312	0,8245
5	0,2095	0,0762	0,8209	0,8245
6 (best)	0,0339	0,0339	0,4380	0,8245

Six options of the track condition allow generating irregularities of different quality. The Lmin and Lmax parameters specify the minimal and the maximal length of irregularity in the realization (m).

PSD functions of the six classes are the following:

- PSD of half-sum of horizontal track irregularities:

$$\phi(\Omega) = \frac{A_\alpha . \Omega^2}{\Omega^2 . (\Omega^2 + \Omega_c^2)}, \quad \Omega > 0 \qquad (2.2)$$

Ω = circular frequency, rad/m

- PSD of half-sum of vertical track irregularities:

$$\phi(\Omega) = \frac{A_v.\Omega^2}{\Omega^2.(\Omega^2+\Omega_c^2)}\ ,\ \ \Omega > 0 \qquad (2.3)$$

- PSD of half-difference of horizontal track irregularities:

$$\phi(\Omega) = \frac{4.A_v.\Omega_c^2}{(\Omega^2+\Omega_c^2).(\Omega^2+\Omega_s^2)}\ ,\ \ \Omega > 0 \qquad (2.4)$$

- PSD of half-difference of vertical track irregularities:

$$\phi(\Omega) = \frac{4.A_v.\Omega_c^2}{(\Omega^2+\Omega_c^2).(\Omega^2+\Omega_s^2)}\ ,\ \ \Omega > 0 \qquad (2.5)$$

2.3. Wheel-Rail Contact

This section consists of general information about the wheelset, the contact area of a vehicle system, creep forces and kalker term, rolling radius difference, oscillation and kinematics of the wheelset on a curve.

2.3.1. Wheelset

A wheelset consists of two wheels and an axle with a rigid contact. The wheelset provides the distance between the rail and the vehicle. In addition, the wheelset supplies the guidance and transmittes traction and breaking forces to the rail to accelerate and decelerate the vehicle.

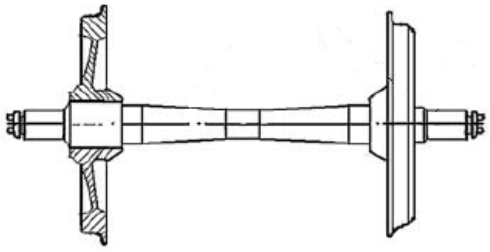

Figure 2.3.1. The wheelset

The major factor that specifies the motion of a wheelset is wheel profile. The wheel profile is determined on the basis of vehicle speed, vehicle mass, rail profile of line and curvature of track. The wheel profile consists of flange, tread and chamfer parts as shown in figure 2.3.2. The position of the contact point when the wheelset is at a central position on the rails is called tape circle.

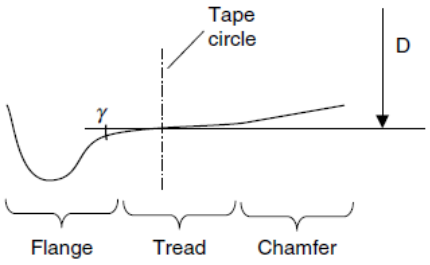

Figure 2.3.2. Main elements of a wheel profile

In the dynamic behaviour of a railway vehicle, the conicity of interface is important. Conicity is defined as the difference in rolling radius between the wheels for a given lateral shift of the wheelset. Conicity suppplies an easy rotation in a curve and it is denoted as γ. The flange located inside the wheel prevents derailment and provides guidance. The equivalent conicity (γ_{eq}) is the ratio of difference in diameter between wheels (ΔR) to the axle length (2y). The following equation shows that the equivalent conicity depends on both wheel and rail profile.

$$\gamma_{eq} = \frac{\Delta R}{2y} \tag{2.6}$$

Despite the variety of wheel profiles, they have a number of common features. The width of the profile is typically 125 – 135 mm and flange height for vehicles is typically 28 – 30 mm. The flange inclination angle is normally between 65 and 70°. In vicinity of the tape circle, the conicity is 1:10 or 1:20 for common rolling stock. For high speed vehicle, the conicity is reduced to around 1:40 or 1:50 to prevent hunting.

The wear which occurs in rolling plane of the wheel profile will increase the height of the flange. The tough flanging appears and more load is implemented to the rail joint bars. Flange wear may lead to increase of the flange angle and reduction of the flange thickness.

2.3.2. The contact area

The linearization of wheel rail contact is get easier with using Hertz spring. In this way, the springs are adapted in such an irregular track. That is why this method is called as Adaptive Contact Method. In standard vehicles, the stifness of spring is described according to properties of wheels. However in this way, the stifness changes according

to properties of rail's and wheel's material and geometry. The study of the contact between bodies is possible today with finite element methods. However, the necessity to calculate as quickly as possible in the dynamic codes leads to the use of analytical methods.

The forces are transmitted by means of the contact area during wheel rail contact. Here, the equation between the contact force (F) and the contact area (y) is given as follows [7]:

$$F = ch.y^{3/2} \tag{2.7}$$

where c_h [Nm-3/2] is a constant related to properties of material and radius. The Wheel rail contact should be defined linearly to set up a linear model. Therefore, this contact problem may be linearized by using a Hertz spring related to contact force and a displacement increment related to static wheel load.

The movement of the wheel on the rail is observed in 4 different contact points :

(a) Wheel-chamfer point
(b) Wheel-tread point
(c) Flange transition
(d) Flange

2.3.3. Creep, creep coefficients and creep forces

Creep is defined as a small apparent slip due to the difference between the tangential strains in the two bodies. When a wheel deviates from pure rolling (during traction, braking or curving) 'creepage' or microslip in the contact patch occurs due to the different velocity of material in the wheel and the rail.

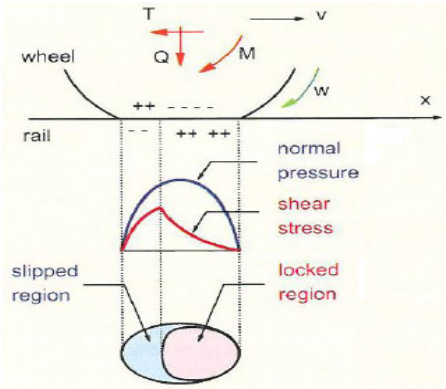

Figure 2.3.3. Explanation of creep phenomenon [8]

As shown in figure 2.3.3, the contact elipse that occurs during wheel rail contact is researched into two parts which are slipped and locked regions. The size of these regions affects the creep forces and the dynamics of rail vehicle. The structure and size of these regions are specified by the wheel rail contact shape and wheel rail profile. For example if two spherical bodies start to roll on each other, the contact elipse becomes circular.

In vehicle dynamics, small creep values have main importance. The longitudinal and lateral creep as well as spin should be taken into account. Typical shapes of measured creep force and creep functions for large creep are shown in figure 2.3.4. The form and the initial slope for wet, dry or polluted conditions are different.

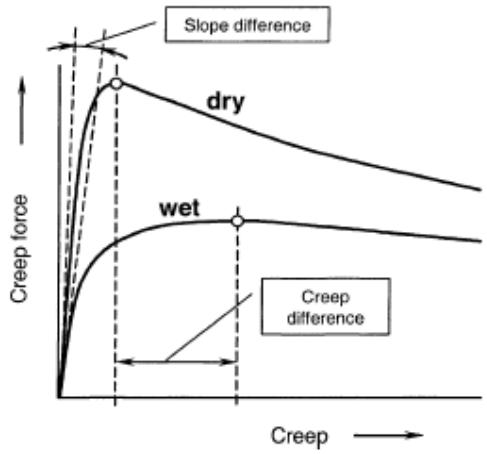

Figure 2.3.4. Typical shape of measured of creep force

A solid axle railway wheelset with both the wheels fixed with the axle is shown in figure 2.3.5. Both the wheels have profiled tread with the conicity γ. This coned tread provides a natural feedback (due to the difference in the rolling radius) for the wheelset to adjust itself on the centre position when it is slightly displaced laterally. The motions of the wheelset are governed by the nonlinear creep forces generated at the wheel rail contact patch in the lateral and longitudinal directions.

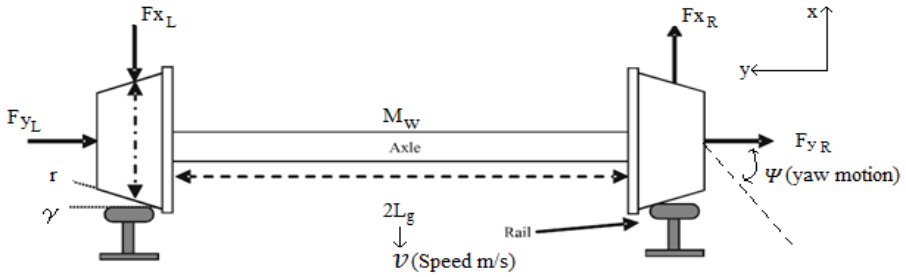

Figure 2.3.5. Creep forces on wheelset

Only lateral and yaw dynamics are found to be sufficient to identify the track condition. The yaw angle is the result of the difference in the longitudinal creep forces between the two wheels and the lateral dynamics are determined by the total creep force of the two wheels in the lateral direction. The relationship for the lateral and the yaw motions of the railway wheelset according to figure 2.3.5 are given below:

$$m_w \ddot{y} = -F_{yR} - F_{yL} + F_C \tag{2.8a}$$

$$I_w \ddot{\Psi} = F_{xR} L_g - F_{xL} L_g - k_w \Psi \tag{2.8b}$$

where m_w is the wheelset mass, F_c is the centrifugal component of the force and can be ignored if the wheelset is not running on the curved track, I_w is the yaw moment of inertia and kw is the yaw stiffness of a spring used to stabilise the wheelset. F_{yL}, F_{yR}, F_{xL} and F_{xR} are the creep forces of left and right wheels in lateral and longitudinal directions.

The creep forces appear from wheel rail profile with results of relation between the wheel and the rail. The creep forces are widely recognised to present the non-linear characteristics as a function of creep.

In the case of a Hertzian contact, the creep forces are a function of the relative speeds between rigid bodies near the contact point, the creepages. The general expression of the creep forces takes into account stiffness coefficients expressed in the linear theory of Kalker [21] by:

$$F_x = -f_{33}\xi_x \tag{2.9a}$$

$$F_Y = -f_{11}\xi_Y - f_{12}\xi_{SP} \tag{2.9b}$$

$$M_Z = -f_{12}\xi_Y - f_{22}\xi_{SP} \tag{2.9c}$$

where ξ_x, ξ_Y and ξ_{SP} are longitudinal, lateral and spin creepages of wheels respectively. These terms may change according to wheelset's speed, wheels' conicity, rolling radius and axle length.

As shown in equation (2.9), creep forces are calculated with the multiplication of creepages and creep coefficients. Here, the force in the direction of longitudinal and lateral, and the moment in the vertical direction occur. The creep coefficients are expressed by f_{11}, f_{12}, f_{22} and f_{33}. These terms covary with the size of contact point, rolling radius and material properties of wheel and rail.

2.3.4. Kalker factor term

Kalker factor represents the scaling factor applied to the Kalker coefficients. The scaling factor is related with the size $c = \sqrt{ab}$ of the contact elipse between wheel and rail. In the case of a Hertzian contact, the creep forces are a function of the relative speeds between rigid bodies near the contact point, the creepages. The general expression of the creep forces takes into account stiffness coefficients c_{ij} expressed in the linear theory of Kalker [21] by:

$$F_x = -Gabc_{11}v_x \tag{2.10a}$$

$$F_{y_{yaw}} = -Gabc_{22}v_y \tag{2.10b}$$

$$F_{y_{spin}} = Gabc_{23}c\varphi \text{ (with } c = \sqrt{ab}\text{)} \tag{2.10c}$$

where G is the material shear modulus (steel in the railway case); πab is the contact ellipse surface; and c_{ij} are the coefficients. In this study, when expressing the equations

of motion of wheelset, the creep coefficients values [28] have been taken in accordance with the Kalker factor term (0.5) which was used in ADAMS/Rail software. In software, the kalker factor terms change between 0.5 and 1.0, and it specifies the limits of creep coefficients. The creep coefficients are:

- f_{11}= 9.430 E6 N
- f_{12}= 23730 N-m
- f_{22}= 66.11 N-m^2
- f_{33}= 10.23 E6 N

2.3.5. Oscillation of wheelset

The wheelset makes a kinematic oscillation on a straight track because of wheel profile's conicity, track irregularity and geometrical run-out. This oscillation is defined in two main degrees of freedom which are lateral displacement (y) and yaw angle (Ψ) as shown in figure 2.3.6.

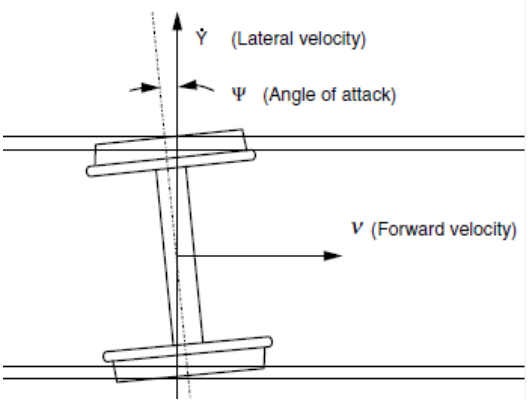

Figure 2.3.6. Yaw motion

Kinematic oscillation was first analysed mathematically for the case of purely coned wheels by Klingel [3] in 1883, who showed that the frequency of oscillation is proportional to speed and to the square root of the cone angle. Klingel's description of wheelset oscillation assumes that pure rolling is maintained throughout the motion of the wheelset. Klingel formulated the first mathematical analysis of the kinematic oscillation of the conical wheelset. Freely rolling wheelsets perform a sinusoidal motion. Klingel derived the relationship between the wavelength L_k the wheelset conicity γ, wheel radius r, and the lateral distance between contact points s as

$$L_k = 2\pi\sqrt{\frac{rs}{2\gamma}} \tag{2.11}$$

As the vehicle speed is increased, so is the frequency of kinematic oscillation. The speed v is equal to multiplication of frequency f and the wavelength L_k.

$$f = \frac{v}{L_k} \tag{2.12}$$

The Klingel movement is dependent only on track and wheelset geometric characteristics, and represents a global effect of wheel–rail interaction. If the frequency f is close to one of the natural frequencies of the wheelset, the periodic movement could cause the vehicle instability. The lateral accelerations on the wheelset due to Klingel movement are described by the ratio v/L_k [3]:

$$\ddot{y} = 4\pi^2 y_0 \left(\frac{v}{L_k}\right)^2 \tag{2.13}$$

where y_o is the amplitude of wheelset lateral displacement. At the same speed, a lower conicity γ produces a movement with greater wavelength, but with lower lateral acceleration. Klingel has defined kinematic oscillation without bothering the effects of creep forces. The creep forces as a result of wheel rail contact change the kinematic oscillation of wheelset.

2.3.6. Rolling radius difference

The rolling radius difference as a result of motion of wheelset in y direction is related to rail profile and the conicity of wheel profile. When the conical wheel runs on the circular rail without flange contact, there is only one contact point between the wheel and rail profiles, as shown in figure 2.3.7.

In the central position of the wheelset, due to the symmetry of the wheelset/track system, the rolling radius r and r_1, r_2 for the right and left wheels are equal. If the wheelset centre is displaced for quantity Δy, then the rolling radius due to conicity of the wheels will be different for the right and left wheels, creating rolling radius difference $\Delta r = r_1 - r_2$.

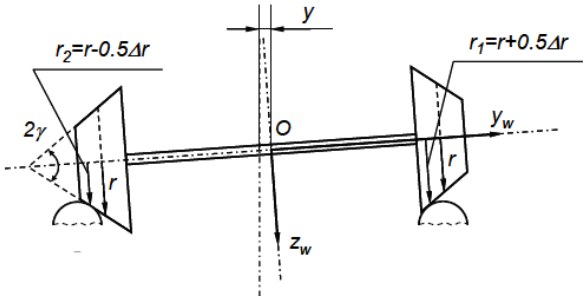

Figure 2.3.7. Rolling radius corresponding to wheelset displacement [9]

The contact point identifies the rolling radius. The radius difference between two wheels is defined as rolling radius difference and the kinematic oscillation of wheelset is considered functionally.

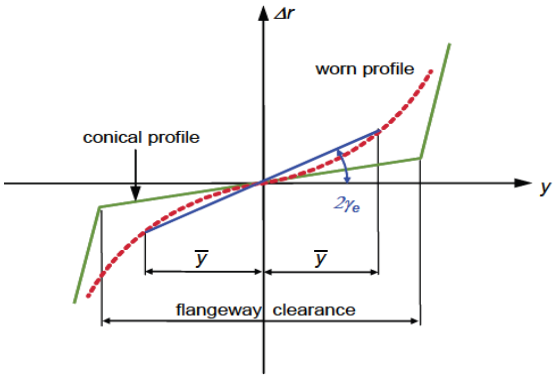

Figure 2.3.8. Rolling radius difference functions [9]

2.3.7. Kinematics of a Wheelset on Curved Track

The required rolling radius difference in wheelset for passing a curve without slippage is highly important. Therefore, the curvatures which the vehicle moves on affect the conicity of wheelset.

A simple geometric relationship between the outward movement of wheelset y , the radius of the curve R , the wheel radius r , the distance between the contact points $2b$ and the conicity γ of the wheels can be derived in order to obtain pure rolling as shown in figure 2.3.9:

$$\frac{\Delta+dr}{\Delta-dr} = \frac{R+b}{R-b} \tag{2.14}$$

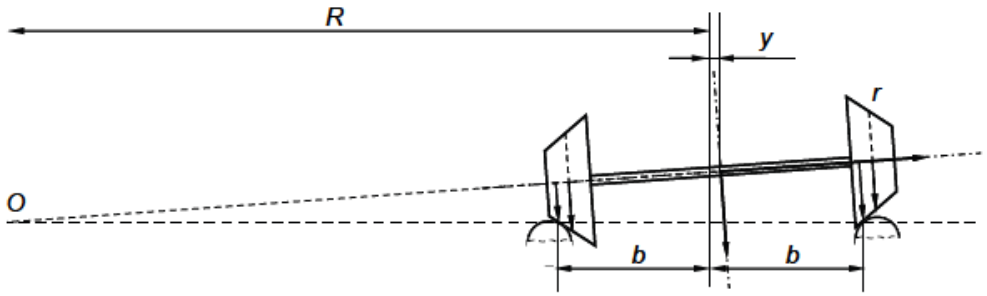

Figure 2.3.9. Rolling of a coned wheelset in curve [13]

Therefore, the required rolling radii difference in wheelset for passing a curve without slippage can be calculated according to the formula

$$\Delta r = \frac{2br}{R} \tag{2.15}$$

The relationship between lateral displacement y of the wheelset and curve radius R can be derived as follows:

$$y = \frac{rb}{\gamma R} \tag{2.16}$$

The application of Redtenbacher's formula [6] shows that a wheelset will be able to move outwards to achieve pure rolling only if either the radius of curvature or the flangeway clearance is sufficiently large. Otherwise, a realistic consideration of curving requires analysis of the forces acting between the vehicle and the track.

2.4. Wheelset Modeling

In this section, railway vehicle model similar to UM models of railway vehicles is presented. The vehicle is considered as a system of rigid or flexible bodies connected by means of joints and force elements. A simplified model of loco E43000 is described. The bodies in models were created in ADAMS/Rail programme with drawings, documentation and photos.

The model of wheelset with 6 degrees of freedom includes two bodies, two joints and a wheelset image is shown in figure 2.4.1. The coordinates of the wheelset are numbered in the following sequence:

1- Transition X
2- Transition Y
3- Transition Z
4- Rotation Z
5- Rotation Y
6- Rotation X

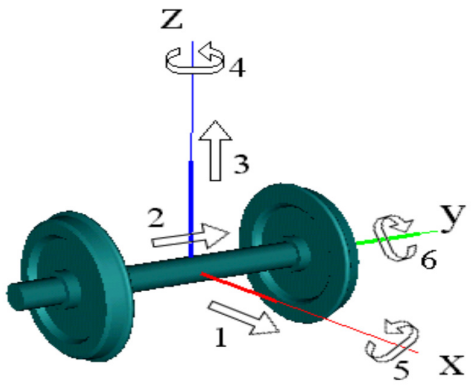

Figure 2.4.1. Wheelset degrees of freedom

Geometrical properties of a wheelset are fully set with the following data: wheelset semibase (L/2), running circle radius (r), reduction of running circles radii d_r and wheel profiles for the left and right wheels, which should be given in a special coordinate system of profile. Figure 2.4.2 and 2.4.3 show the geometrical parameters of wheelset and system of coordinates of a wheel profile respectively.

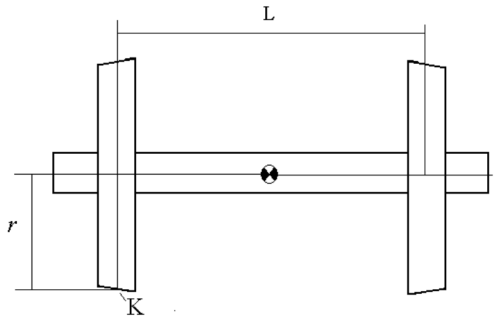

Figure 2.4.2. Geometrical parameters of wheelset

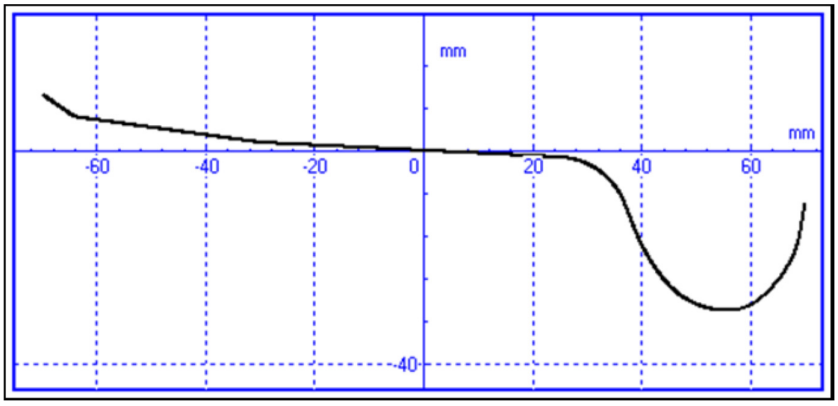

Figure 2.4.3. System of coordinates of a wheel profile

Figure 2.4.4 shows the single wheelset modeling which modified in ADAMS/Rail. There are several parameters to create the model. Tape circle distance, axle length, rolling radius, mass of wheelset, moments of inertia and properties of right and left wheels affect the dynamic behaviour of the vehicle.

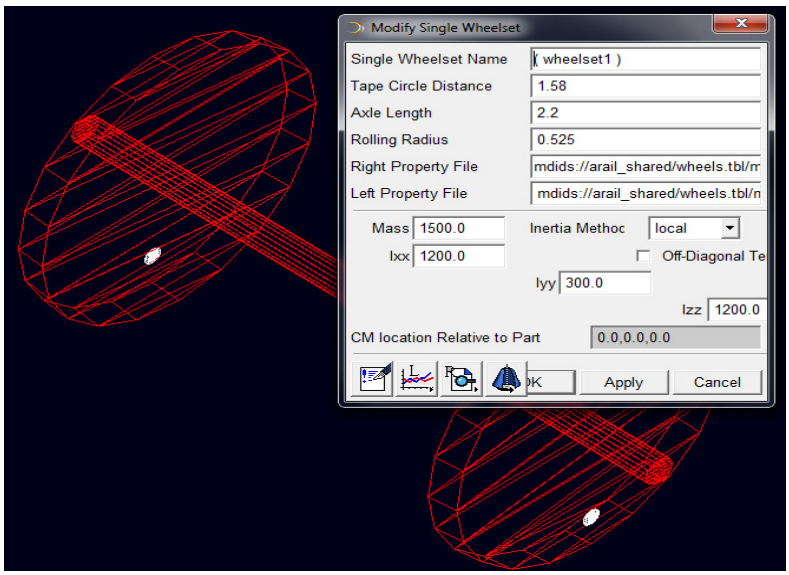

Figure 2.4.4. Modeling of wheelset in ADAMS/Rail

2.5. Bogie Modeling

The bogie system has been generated by two wheelset, four axle boxes and a bogie frame. A locomotive bogie has 22 degrees of freedom totally. These degrees of freedom are numbered in the following sequence as seen in figure 2.6.2.

- The front wheelset has 6 degrees of freedom (transition and rotation in x,y,z)
- The rear wheelset has 6 degrees of freedom (transition and rotation in x,y,z)
- The bogie frame has 6 degrees of freedom (transition and rotation in x,y,z)
- The four axle boxes have 1 degree of freedom (rotation in y).

The locomotive bogie which has been created in ADAMS/Rail (figure 2.5.2) is similar to the E43000 locomotive bogie (figure 2.5.1) which was made by TRENSIM project [12] for Turkish State Railways.

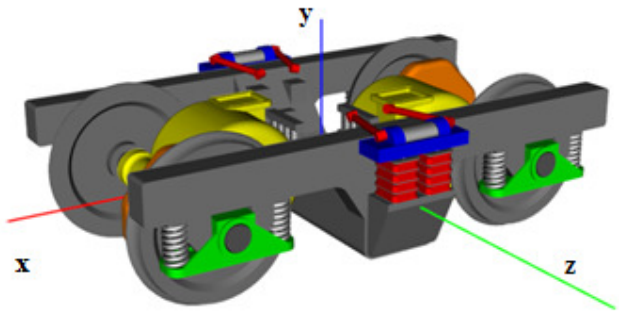

Figure 2.5.1. E43000 locomotive bogie [14]

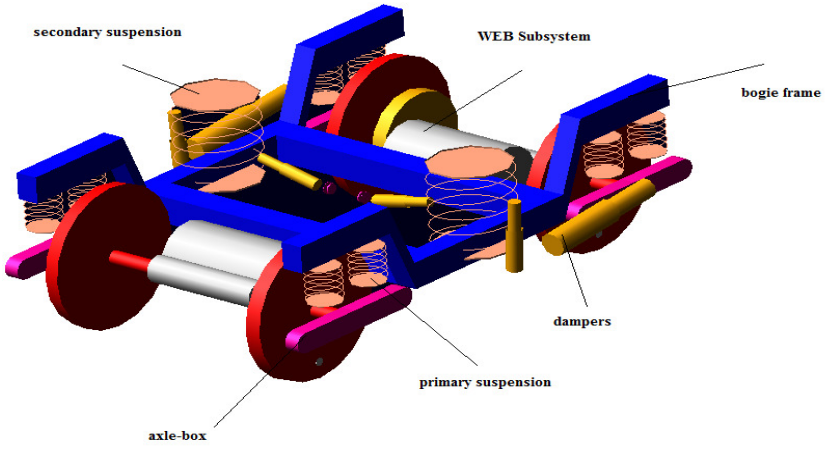

Figure 2.5.2. E43000 locomotive bogie in ADAMS/Rail

2.5.1. Axle-boxes

Most bogies have two axles. The side frame of the bogie was usually of bar construction, with simple horn guides attached, allowing the axle boxes vertical movements between them. The axle boxes had a cast-steel equaliser beam or bar resting

on them. The bar had two steel coil springs placed on it and the bogie frame rested on the springs. The effect was to allow the bar to act as a compensating lever between the two axles and to use both springs to soften shocks from either axle.

Axle box suspensions absorb shocks between the axle bearings and the bogie frame. The axle box suspension usually consists of a spring between the bogie frame and axle bearings to permit up-and-down movement, and sliders to prevent lateral movement. A more modern design uses solid rubber springs.

Sometimes axle-boxes are not included in vehicle models as separate bodies and the bogie frame is connected directly with the base of the wheelset. In this case graphic images of axle-boxes can be introduced to make the vehicle model more realistic. The images of the axle-boxes are assigned to the base of the wheelset. In other cases introduction of axle-boxes as separate rigid bodies is necessary to make the model correct. Some of these cases are listed below.

- Non-symmetric attachment and different stiffness of a pair of springs connected with the axle-box.
- Non-symmetric attachment of traction rods for traction wheelset;
- Lateral gaps in axle-box assembly for some locomotives with 3 axle bogies.

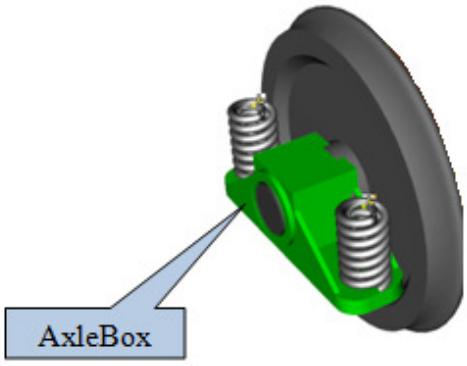

Figure 2.5.3. A wheel with an axle-box

An axlebox consists of the following objects:

- One part with its geometry representing the axlebox.
- A variable storing the global position.
- Two variables used for the geometric parameters calculation.

In ADAMS/Rail, it creates the part in such a way so as to have the same location and orientation as the reference frame. You can express the center of mass (CM) location in the part local reference frame. The orientation is always equal to the part orientation. To create an axlebox element in the Template Builder, it can specify the following parameters:

- Reference frame defining the position and the orientation of the part and its geometry
- CM location relative to part (in three directions: x, y, and z)
- Mass and inertia properties of the axlebox parts
- Axlebox type
- Axlebox width
- Front link length
- Front link height
- Rear link length
- Rear link height

2.5.2. Primary and secondary suspensions

Almost all railway vehicles use bogies to carry and guide the body along the track. Bogie suspension design is a complex and difficult science which has evolved over many years. It was recognised very early in the development of railways that the interface between vehicle body and wheel needed some sort of cushion system to reduce the vibration felt as the train moved along the line. This was already part of road coach design and took the form of leaf (laminated) steel springs mounted on the axles, upon which the vehicle body rested. The natural progression from the rigid framed vehicles used in the early days of European railways to a bogie vehicle brought with it a more sophisticated suspension system. This system was based on a steel plate framed bogie with laminated spring axlebox suspension, much as seen on the first vehicles, and with a secondary suspension added between the car body and the bogie. Primary and secondary suspensions of a locomotive bogie are shown in figure 2.5.4.

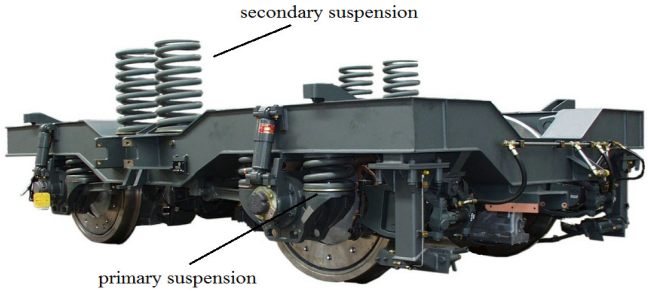

Figure 2.5.4. Primary and secondary suspension of a locomotive bogie

The primary suspensions are composed of chevron springs which are situated on the axle-box. When the bogie frame is located on these suspensions, the loading capacity of the vehicle the mechanical efficiency of the engine increase.

The secondary suspensions are located between the bogie frame and the car body. The air spring which is the basis of secondary suspensions enhances the loading capacity of the vehicle and supplies a ground clearance with a fixed platform.

In ADAMS/Rail, before creating the suspensions for the bogie, it is necessary to create the mount part that connects to the wagon part during assembly. A mount part is a mass less part, fixed to ground by default. This mount part represents the wagon part and acts as a place holder for it. When it creates a mount part, ADAMS/Rail automatically creates an input communicator for it of class mount. The input communicator requests the name of the part to which the mount part should connect. If ADAMS/Rail finds a matching communicator during assembly, it attaches the mount part to the part that the output communicator indicates. This part can be from another subsystem. If ADAMS/Rail does not find a matching output communicator, the mount part remains fixed to ground. To create a mount part, it necessary to specify a hardpoint and a mount part name. If the hardpoint has a left or right symmetrical twin, ADAMS/Rail creates left and right mount parts and input communicators. Otherwise, it creates a single mount part and a single input communicator.

2.5.3. Dampers

Damping is usually provided in railway vehicle suspension by the use of viscous or friction damping devices. Dry friction results from the relative slip between two rigid

bodies in contact. The friction force can be constant or dependent on the mass of the car body, but always acts to resist the relative motion. Friction force is proportional to friction coefficient μ, pressure between surfaces Q, and contact surface area S. This dependence can be represented by the following formula:

$$F_{dry\ fric} = -\mu SQ\frac{\dot{z}}{|\dot{z}|} = -F_0\frac{\dot{z}}{|\dot{z}|} \tag{2.17}$$

where F_0 is the magnitude of friction force; $\dot{z}$ is the relative velocity of motion; $|\dot{z}|$ is the magnitude of velocity. The minus sign denotes that the friction force is always in the opposite direction to the velocity.

Damping of vibrations can also be obtained by other means such as the introduction of active dampers being controlled proportionally to velocity. A damper is the device that controls oscillations in the primary or secondary suspension of the vehicle by energy dissipation. Friction dampers are the devices that transform the energy of oscillations into the heat energy by dry friction. Friction dampers are mainly used in freight vehicle suspensions due to their low cost and simplicity. Depending on their construction friction dampers may be classified as one of four types: integrated with the elastic element, integrated into the spring suspension, telescopic, and lever.

Figure 2.5.5 shows the vertical and transversal damper elements and secondary suspension (force elements) of UM model.

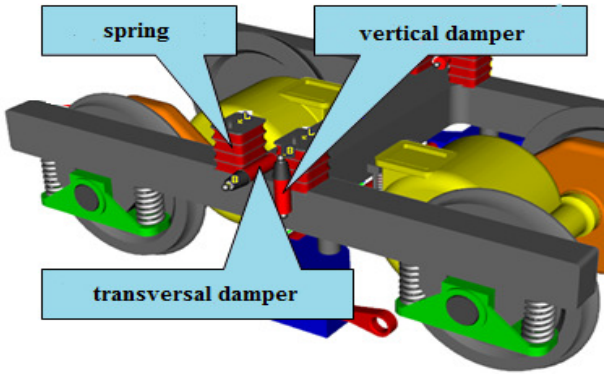

Figure 2.5.5. Force elements of locomotive bogie [14]

2.5.4. Wheelset electromotor block (WEB) subsystem

Wheelset electromotor block (WEB) is a part of bogie of the locomotive which consists of electromotor, wheelset, reducer and axleboxes. The model includes 6 rigid bodies: axlebox right, axlebox left, reducer, engine, rotor, and pinion as seen in figure 2.5.6.

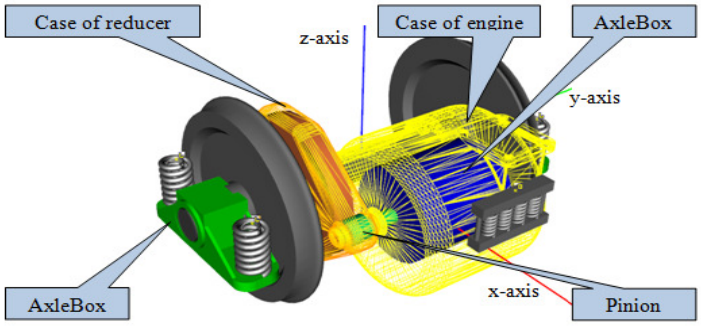

Figure 2.5.6. WEB model [14]

The traditional direct current electric motor driving a train or locomotive is a simple machine consisting of a case containing a fixed electrical part, the stator and a moving electrical part, the rotor or armature as it is often called. As the rotor turns, it turns a pinion which drives a gearwheel. The gear wheel is shrunk onto the axle and thus drives the wheels as shown in figure 2.5.6. The motion of the motor is created by the interaction of the magnetism caused by the currents flowing the the stator and the rotor. This interaction causes the rotor to turn and provide the drive.

2.5.5. Bumpstops

Bumpstops are the devices that limit the relative displacements of bogie units in longitudinal and lateral directions. A bumpstop defines a force-displacement relationship between two parts. The bumpstop acts between user-specified coordinate reference points on each part, and conforms to the force-displacement properties. The bumpstop force is activated when the displacement between the two coordinate references exceeds the clearance defined for the bumpstop. The force-displacement formula is based on:

- Instantaneous distance between the user-specified coordinates defined on each part
- Impact length or clearance
- Bumpstop property file (polynomial or nonlinear stiffness with or without linear or nonlinear damping).

2.6. Locomotive Modeling

In main system, there are three bogie subsystems which are front, middle and rear bogies as seen in figure 2.6.1. The main system has about 70 degrees of freedom in total. In ADAMS/Rail model, the mass of each wheelset electromotor block subsystem has been reduced to the mass of bogie frame.

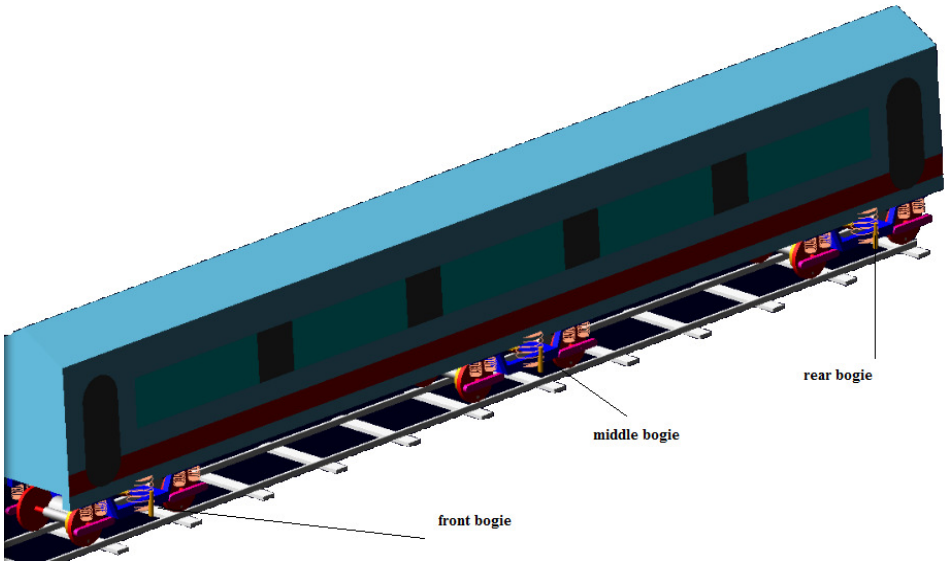

Figure 2.6.1. E43000 locomotive model in ADAMS/Rail

When creating main system, there are major parameters such as wheel radius, conicity, moment of inertia and mass of wheelset, bogie frame and axle-boxes, primary and secondary suspension coefficients. The geometrical and physical parameters of main system are given in table 2.6.1 and shown in figure 2.6.2. Here x,y,z and Θ represents the longitudinal, transversal and vertical transition and rotation of parts. It gives us degrees of freedom of whole system. The whole steps to modify a locomotive model in ADAMS/Rail are given in APPENDIX A.

Table 2.6.1. Geometrical and physical parameters of locomotive model

Parameters	Symbols	Values	Units
Mass of bogie frame	m_2	2719	kg
Moment of inertia of frame (x)	I_{x2}	1.09E+04	kgm^2
Moment of inertia of frame (y)	I_{y2}	9814.886	kgm^2
Moment of inertia of frame (z)	I_{z2}	18900	kgm^2
Mass of wheelset	m_1	1500	kg
Moment of inertia of wheelset (x)	I_{x1}	1200	kgm^2
Moment of inertia of wheelset (y)	I_{y1}	300	kgm^2
Moment of inertia of wheelset (z)	I_{z1}	1200	kgm^2
Mass of axle-box	m_3	201.8	kg
Moment of inertia of axle-box (x)	I_{x3}	4.51	kgm^2
Moment of inertia of axle-box (y)	I_{y3}	15.08	kgm^2
Moment of inertia of axle-box (z)	I_{z3}	13.89	kgm^2
Mass of body	m_4	6.70E+04	kg
Moment of inertia of body (x)	I_x	1.00E+05	kgm^2
Moment of inertia of body (y)	I_y	1.00E+06	kgm^2
Moment of inertia of body (z)	I_z	1.00E+06	kgm^2
Primary suspension longitudinal stiffness	k_{px}	100000	N/m
Primary suspension transversal stiffness	k_{py}	100000	N/m
Primary suspension vertical stiffness	k_{pz}	1000000	N/m
Secondary suspension longitudinal stiffness	k_{sx}	100000	N/m
Secondary suspension transversal stiffness	k_{sy}	100000	N/m

Parameters	Symbols	Values	Units
Secondary suspension vertical stiffness	k_{sz}	1667700	N/m
Traction rod longitudinal stiffness	k_{tx}	10000000	N/m
Traction rod transversal stiffness	k_{ty}	10000000	N/m
Traction rod vertical stiffness	k_{tz}	10000000	N/m
Conicity	γ	0.02	rad
Wheel rolling radius	r	0.525	m
Length of body	l_{bl}	24	m
Height of body	l_{bh}	3	m
Width of body	l_{bw}	2.2	m
Wheelset base	l_b	2.6	m
Lateral width of bogie frame	l_w	2	m
Tape circle distance	l_c	1.58	m
Side frame height	l_{sh}	0.2	m
Side frame width	l_{sw}	0.18	m
Bolster width	l_{bs}	0.2	m
Axle length	l_a	2.2	m
Axle-box width	l_{aw}	0.1	m
Axle-box height	l_{ah}	0.6	m
Cylinder radius	l_{cr}	0.3	m
Cylinder length	l_{cl}	0.6	m
Distance of CM of traction rod to the suspensions	l_{tr}	1	m

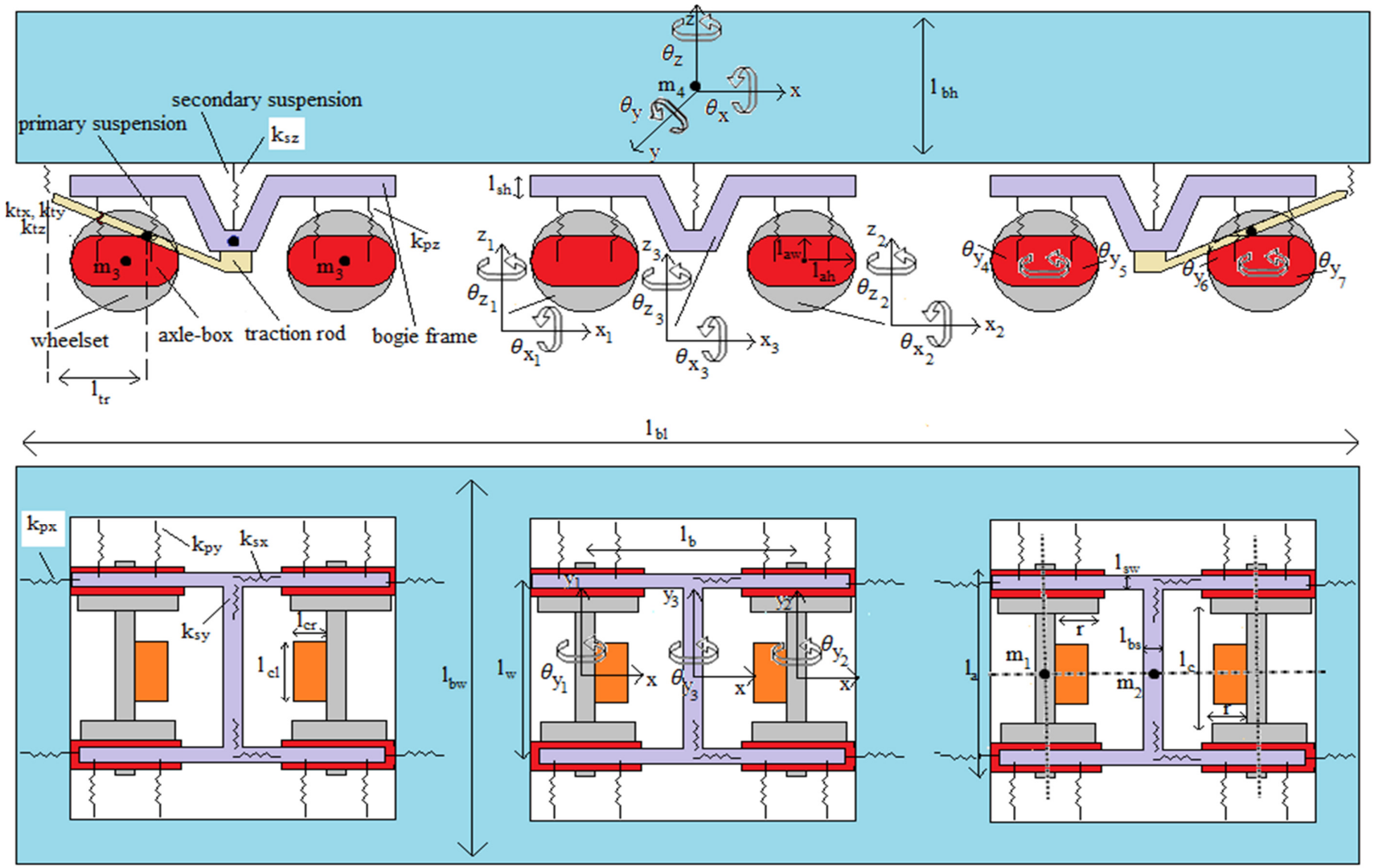

Figure 2.6.2. Side and top view of locomotive model

3. RESULTS AND DISCUSSION

This chapter presents the stability and dynamic analysis results of the models which occured in ADAMS/Rail. The kinematic and dynamic behaviour of wheelset, bogie and locomotive model have been demonstrated and compared with the data of TRENSIM Project.

3.1. Stability Analysis

In figure 3.1.1, the motion of a wheelset on a straight way was investigated and analyzed. The analysis was made for ten different velocity values between 1m/sec and 30 m/sec. The conicity and Kalker factor values has been considered as 0.02 and 0.5 respectively. The critical damping ratio has been considered as zero and the results which are equal to this value have specified the critical speed in ADAMS/Rail.

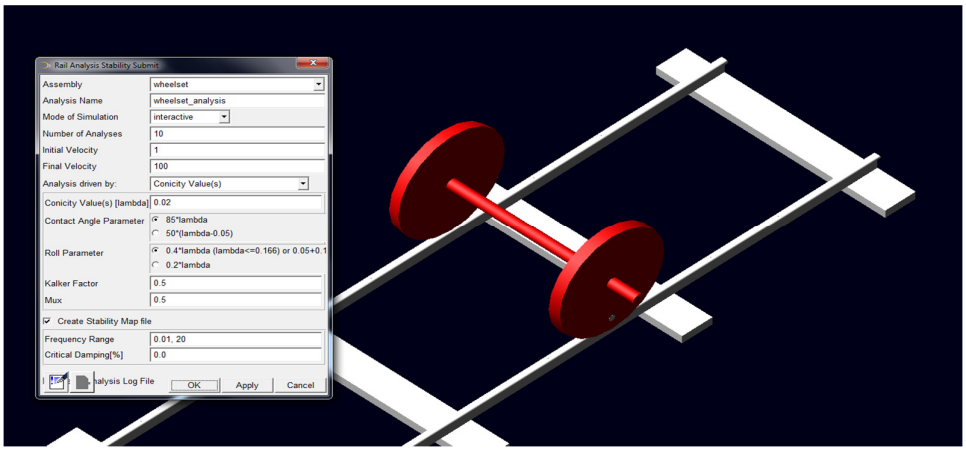

Figure 3.1.1. The motion and analysis of single wheelset on a straight way

The single wheelset model has two degrees of freedom which are lateral motion in y axis and rotational motion in z axis as seen in figure 3.1.2.

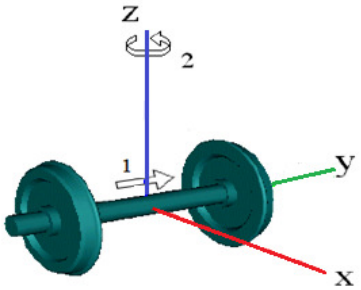

Figure 3.1.2. The degrees of freedom of single wheelset

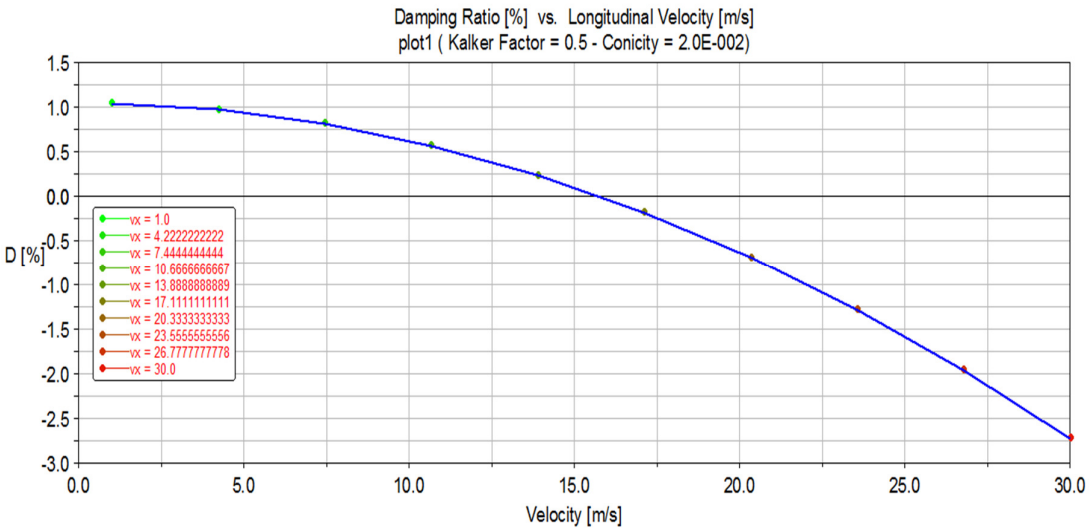

Figure 3.1.3. The damping ratio and longitudinal velocity values of single wheelset

The velocity of single wheelset increases linearly between 0 and 30 m/sec and the damping ratio falls below the critical level (zero) in 16 m/sec (57.6 km/h) as seen in figure 3.1.3. In this speed, the system becomes unstable and the wheelset takes a risk of derailment. This critical speed value shows similarity with the results which were generated with the equations of motion of wheelset (APPENDIX C) in MATLAB.

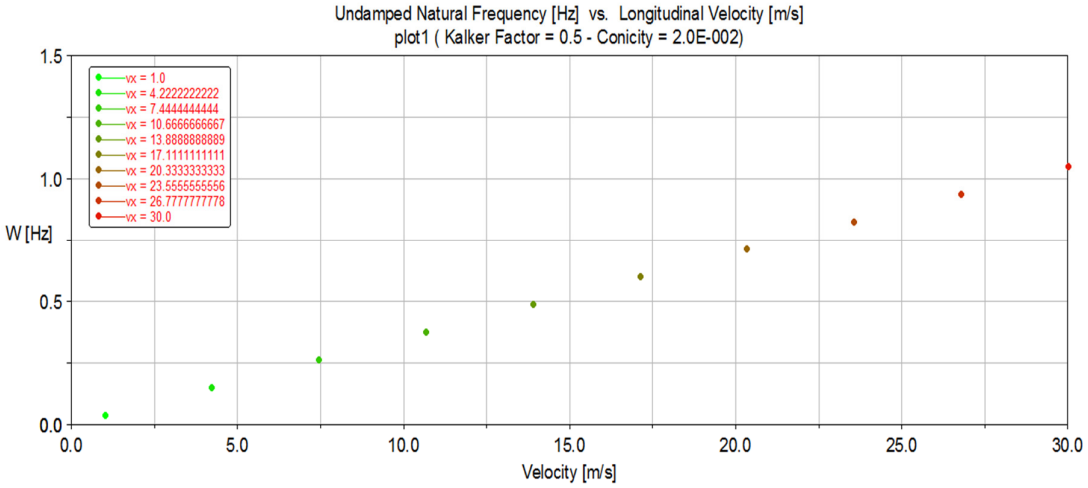

Figure 3.1.4. The natural frequency and longitudinal velocity values of single wheelset

In figure 3.1.4, the natural frequency values are shown with respect to increasing velocity values of single wheelset model on a straight way. The natural frequncy value is about 0.55 Hertz in the critical velocity which has been measured before as 16 m/sec.

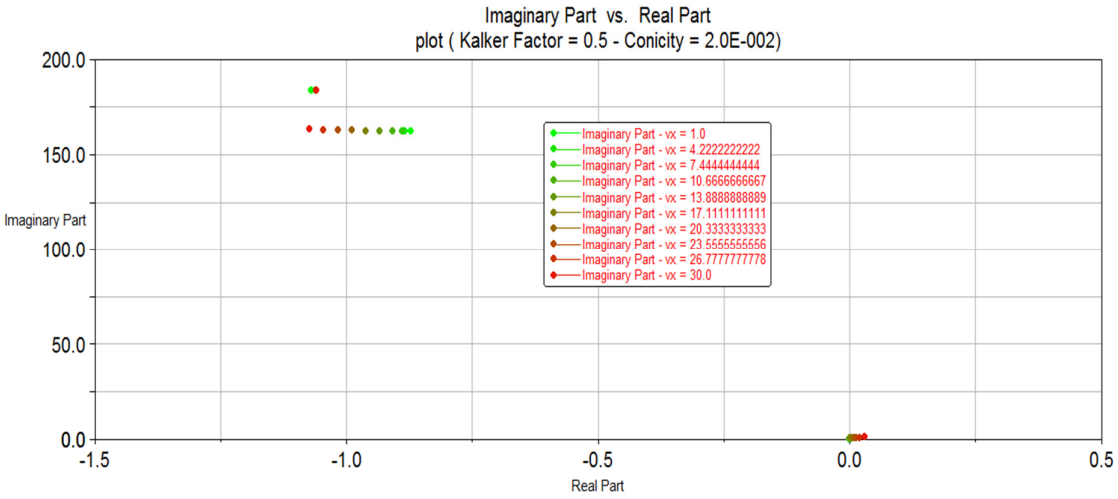

Figure 3.1.5. The eigenvalues of single wheelset in different speeds

In figure 3.1.5, the eigenvalues of single wheelset model has been found for different speeds. The real part of the eigenvalue is positive after the critical speed 16 m/sec and the system has become unstable.

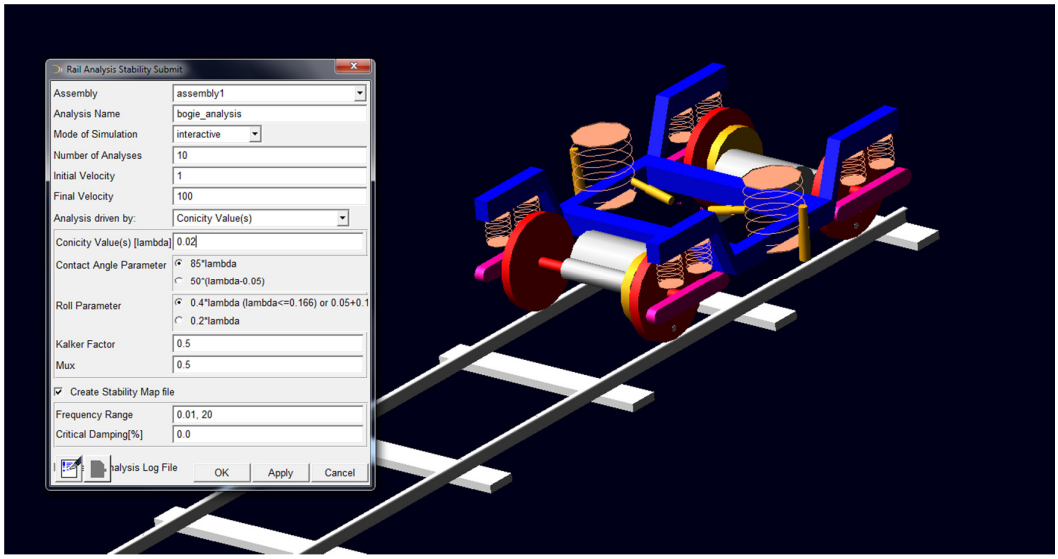

Figure 3.1.6. The motion and analysis of bogie model on a straight way in ADAMS/Rail

The motion and analysis of bogie model which has 22 degrees of freedom is shown in figure 3.1.6. The velocity of bogie model increases linearly between 0 and 100 m/sec with 0.02 conicity and 0.5 Kalker factor with similar to single wheelset model.

The critical speed of bogie model changes according to several parameters such as centre of gravity of wheelset and bogie frame, moment of inertia and creep forces.

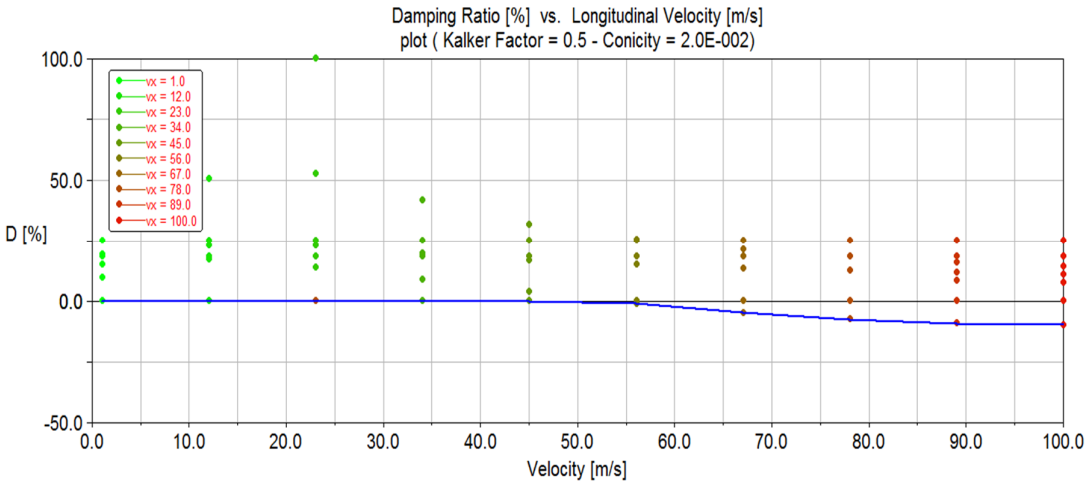

Figure 3.1.7. The damping ratio and longitudinal velocity values of bogie model

The velocity of bogie model increases linearly between 0 and 100 m/sec and the damping ratio falls below the critical level (zero) in 56 m/sec (201.6 km/h) as seen in figure 3.1.7. In this speed, the system becomes unstable and the bogie model takes a risk of derailment.

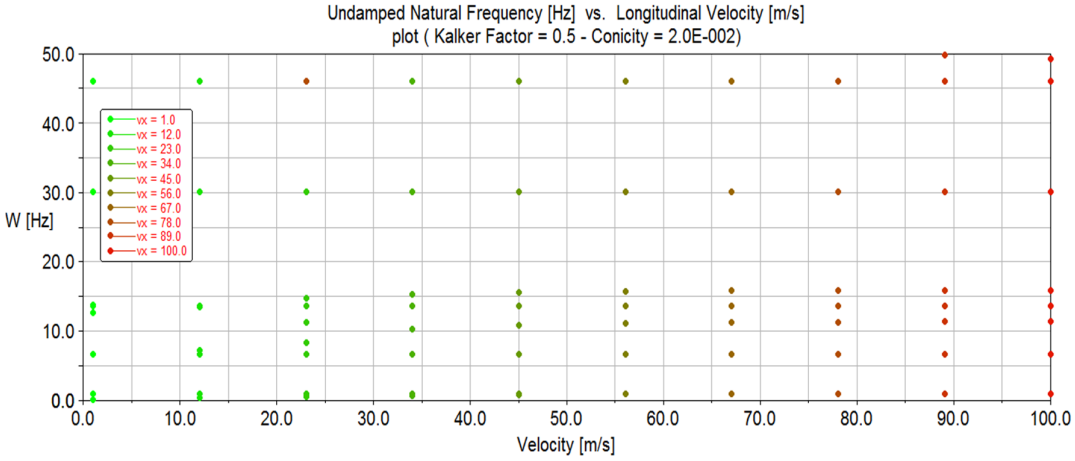

Figure 3.1.8. The natural frequency and longitudinal velocity values of bogie model

In figure 3.1.8, the natural frequency values are shown with respect to increasing velocity values of bogie model on a straight way. The natural frequncy value passes over 45 Hertz value in the critical velocity which has been measured before as 56 m/sec.

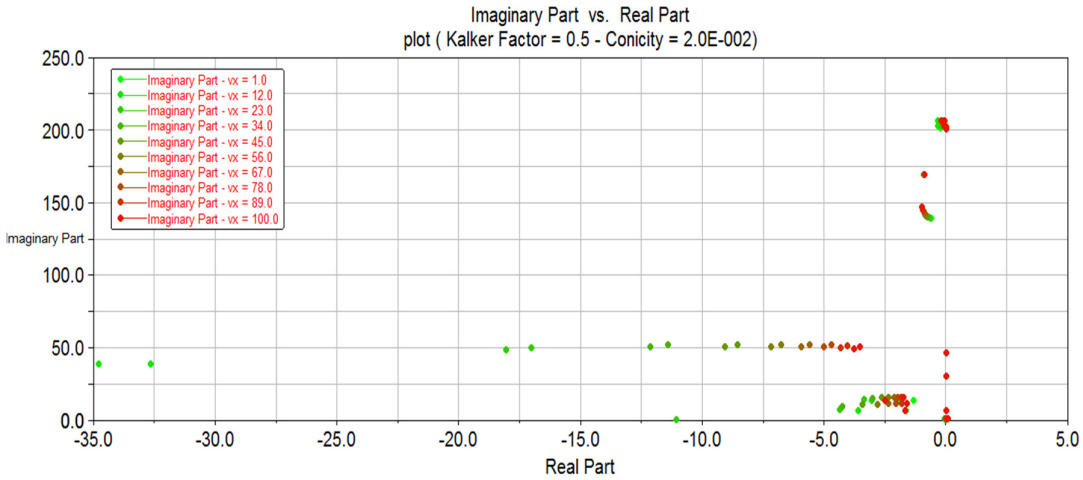

Figure 3.1.9. The eigenvalues of bogie model in different speeds

In figure 3.1.9, the eigenvalues of bogie model has been found for different speeds. The eigenvalues are observed in the positive side of real part which are closed to zero value. It means that the system becomes unstable in high speeds.

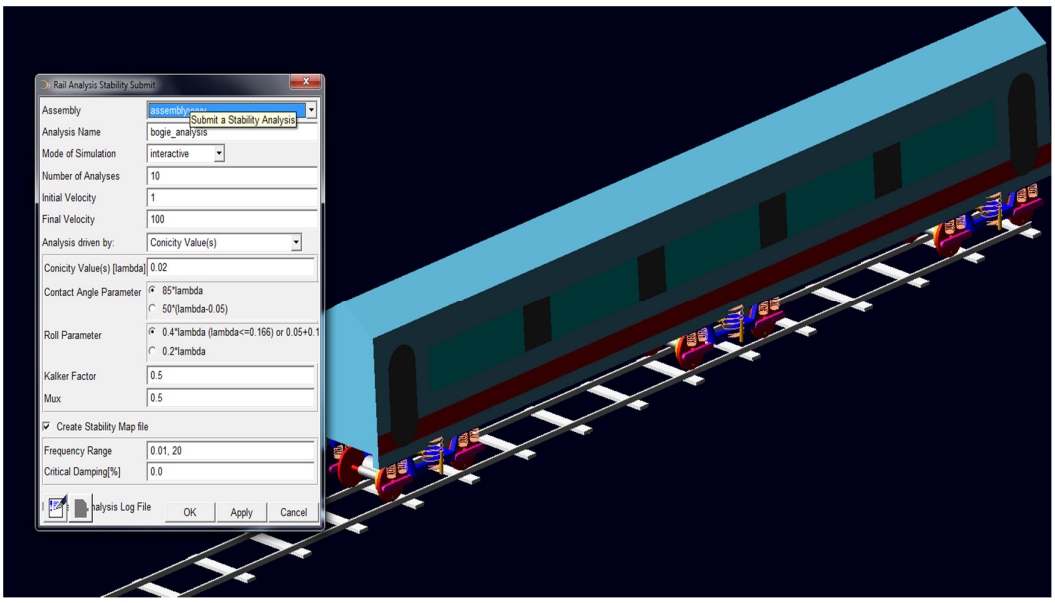

Figure 3.1.10. The motion and analysis of locomotive model on a straight way in ADAMS/Rail

The motion and analysis of locomotive model is shown in figure 3.1.10. The velocity of main model increases linearly between 0 and 100 m/sec with 0.02 conicity and 0.5

Kalker factor and the critical speed of main model is related to mass and moment of inertia of body.

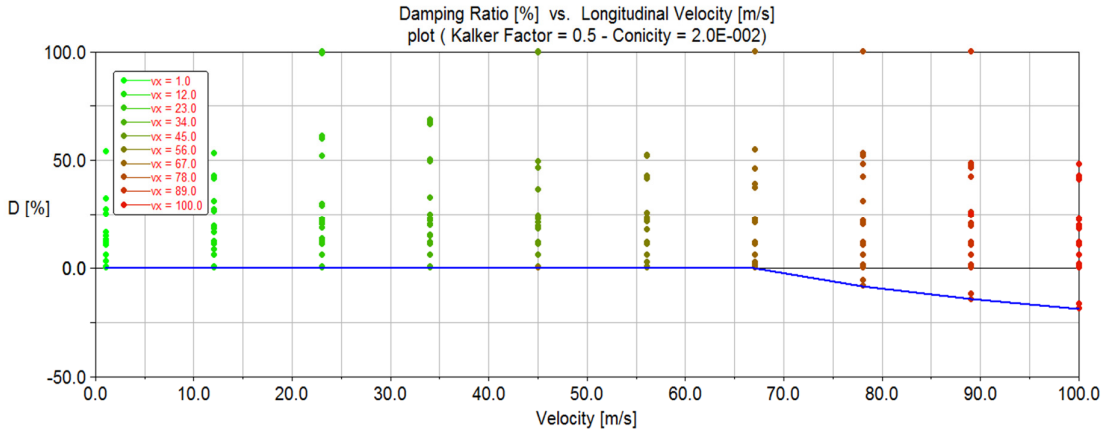

Figure 3.1.11. The damping ratio and longitudinal velocity values of locomotive model

The velocity of locomotive model increases linearly between 0 and 100 m/sec and the damping ratio falls below the critical level (zero) in 67 m/sec (241.2 km/h) as seen in figure 3.1.11. The car body which assembled over three bogie subsystems has increased the critical speed from 56 m/sec to 67 m/sec.

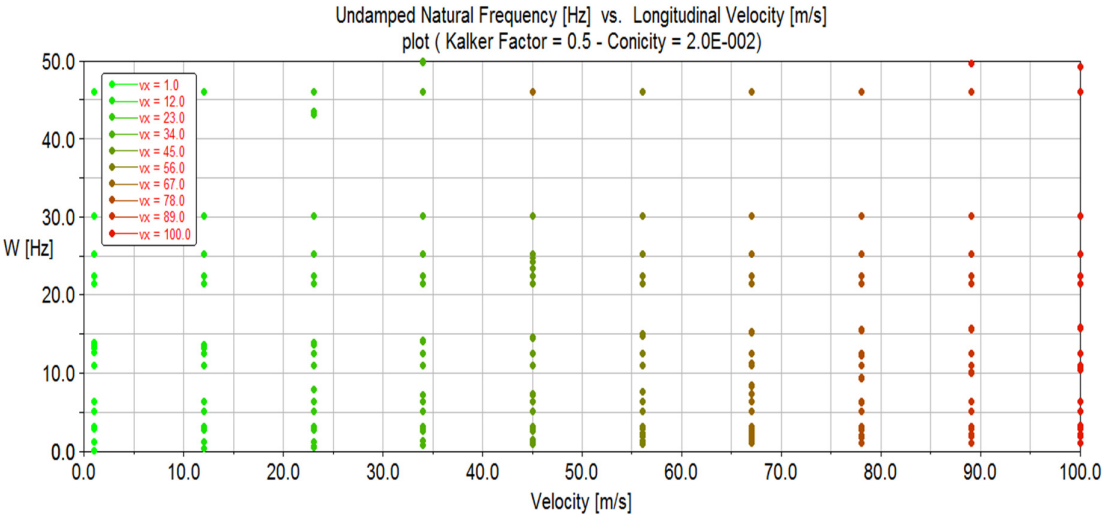

Figure 3.1.12. The natural frequency and longitudinal velocity values of locomotive model

In figure 3.1.12, the natural frequency values are shown with respect to increasing velocity values of main model on a straight way. The natural frequncy value passes over 45 Hertz with similar to analysis of bogie model.

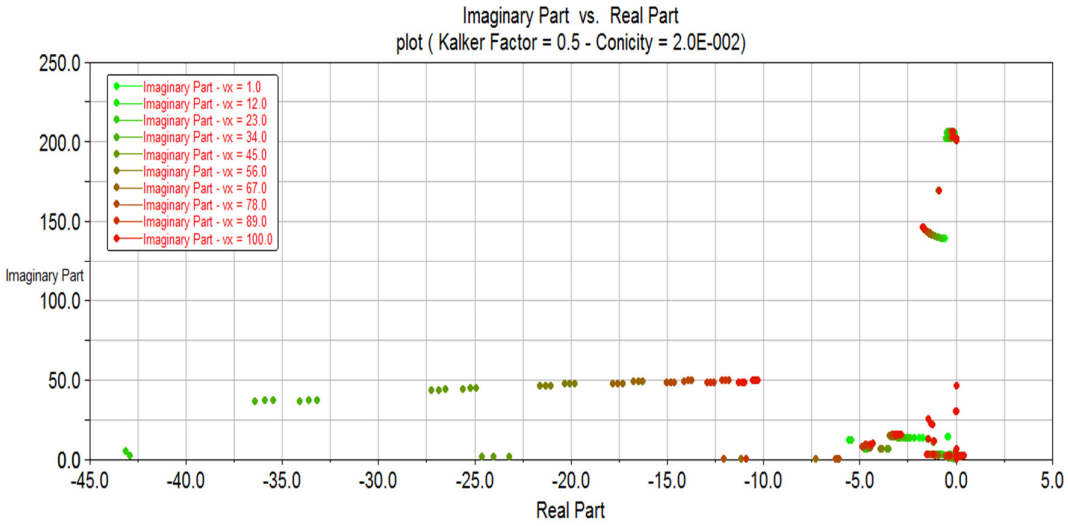

Figure 3.1.13. The eigenvalues of locomotive model in different speeds

In figure 3.1.13, the eigenvalues of main model has been found for different speeds. The eigenvalues are observed in the positive side of real part which are closed to zero value. The real part of the eigenvalue becomes positive after the critical speed 67 m/sec and the system becomes unstable.

3.2 Dynamic Analysis

The dynamic analysis of an experimental wheelset on a straight track which occured in ADAMS/Rail is shown in figure 3.2.1. The vertical oscillation of the wheelset and the second type of random track irregularity have been represented together. The wheelset performs a similar motion depending on track irregularity.

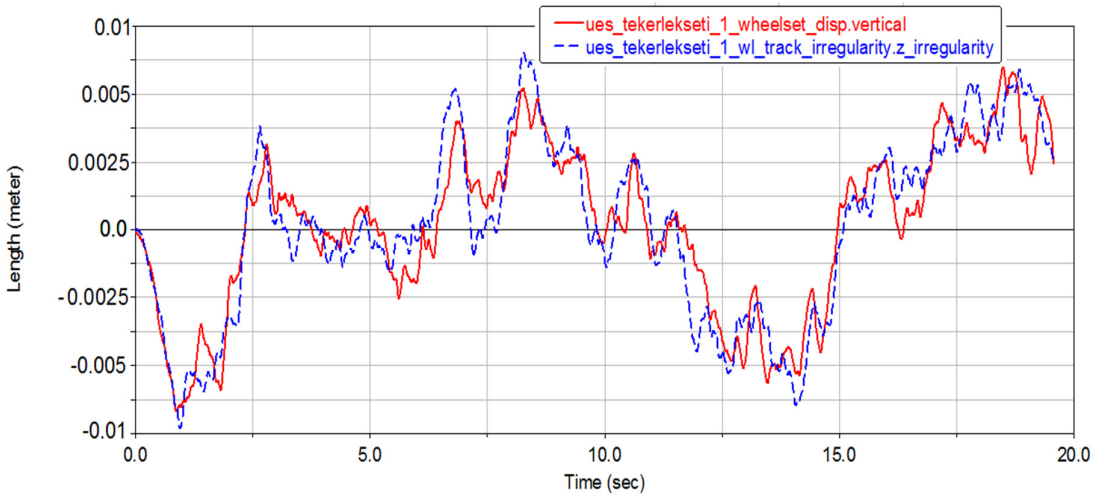

Figure 3.2.1. Vertical displacement of single wheelset and track irregularity in ADAMS/Rail

In figure 3.2.2, the dynamic analysis of a bogie system is shown at a specified point on the frame in ADAMS/Rail. The vertical oscillation of the bogie on the same track irregularity has been compared with the measured data of the bogie in TRENSIM project as seen in figure 3.2.3. In both tests, -15 and +15 milimeter displacements are observed.

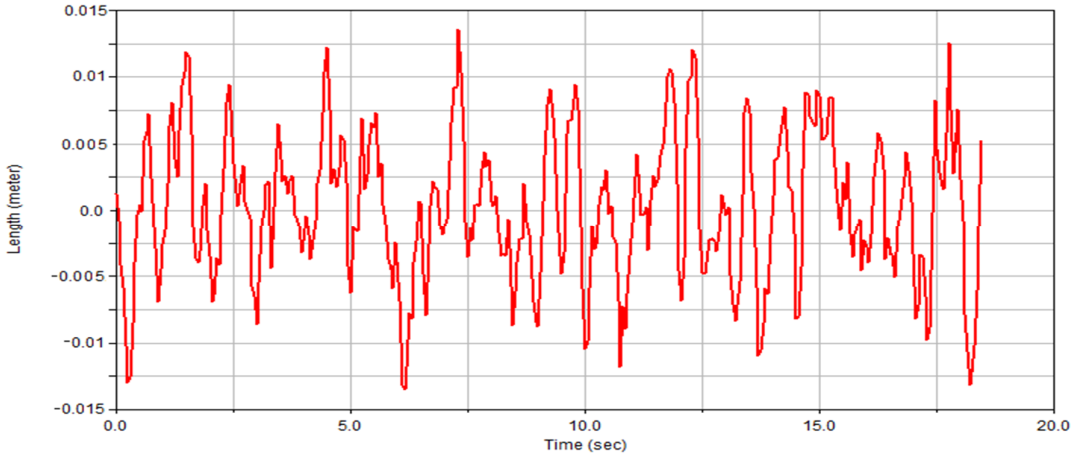

Figure 3.2.2. Vertical displacement of bogie model in ADAMS/Rail

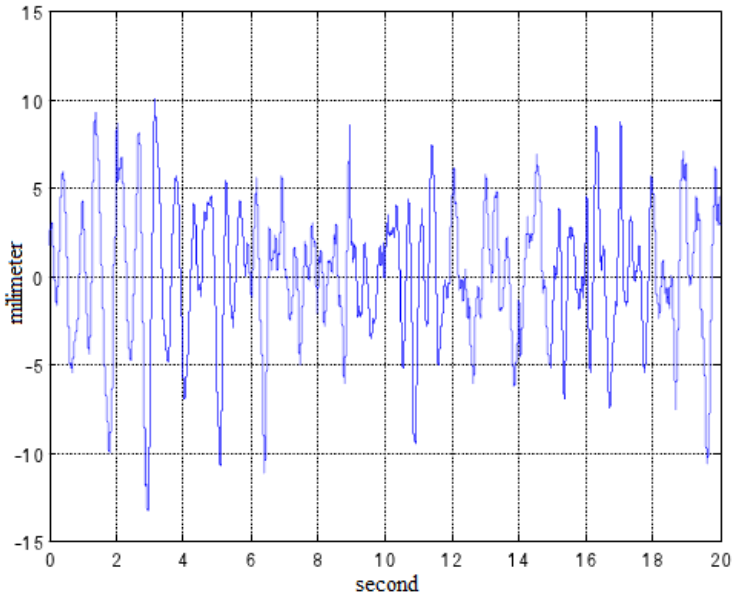

Figure 3.2.3. Vertical displacement of bogie (TRENSIM Project)

In figure 3.2.4, the dynamic analysis of a locomotive model occured in ADAMS/Rail is shown. The vertical oscillation of the locomotive model on the same track irregularity has been compared with the measured data of the locomotive model occured in TRENSIM project as seen in figure 3.2.5. The reference point has been specified one meter below the centre of gravity of the car body.

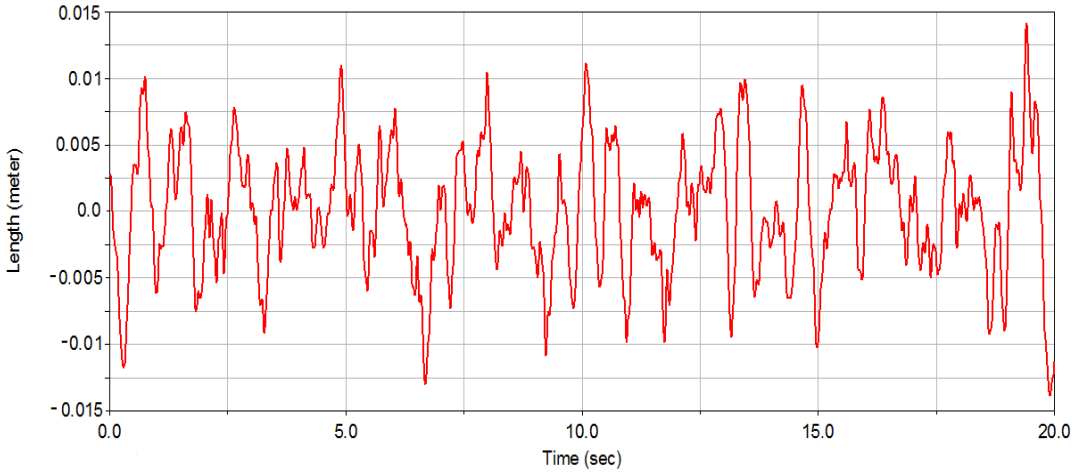

Figure 3.2.4. Vertical displacement of locomotive model in ADAMS/Rail

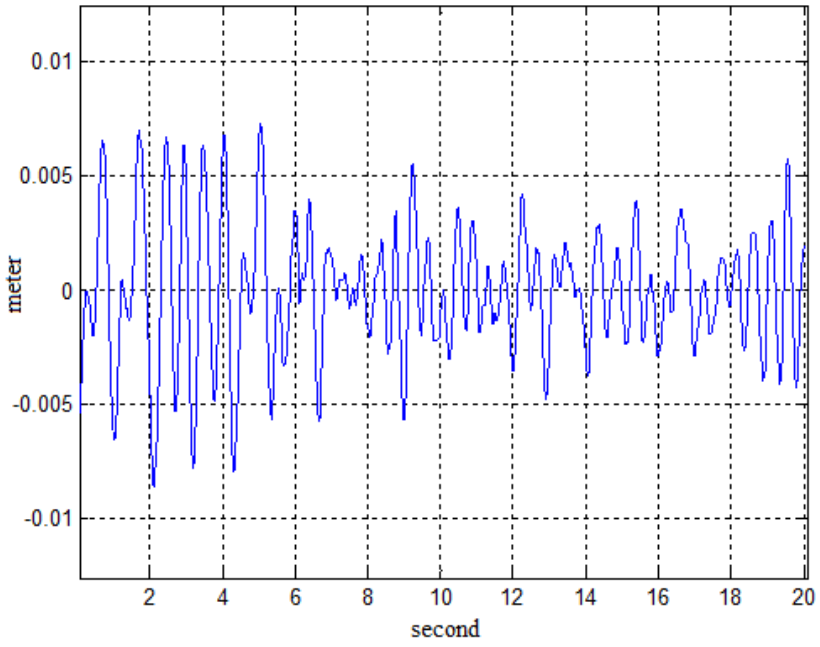

Figure 3.2.5. Vertical displacement of locomotive (TRENSIM Project)

In figure 3.2.6 and 3.2.7, the dynamic analysis results of the single wheelset have been shown on a specified curve which introduced in chapter 2.1. Here, the wheelset has a constant velocity which is 17.5 m/s during the simulation and the track has no irregularities in the lateral or vertical direction. The lateral and vertical displacements have been given respectively. In figure 3.2.6, a small displacement is seen on the circular path. This value shows similarity with the results which were generated with the equations of motion of wheelset as shown in APPENDIX C.

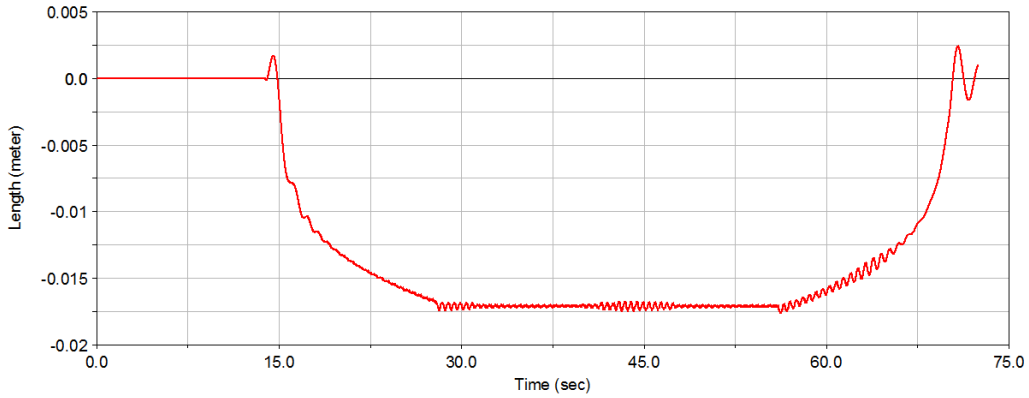

Figure 3.2.6. Lateral displacement of single wheelset on a circular path

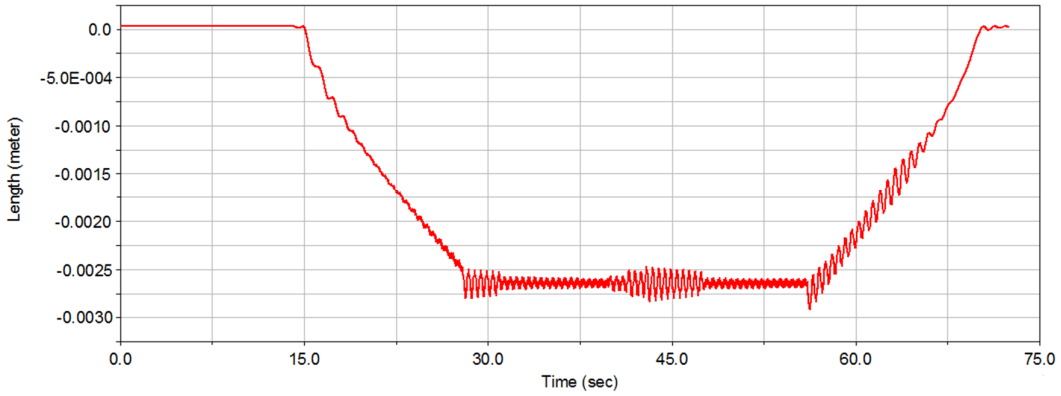

Figure 3.2.7. Vertical displacement of single wheelset on a circular path

In figure 3.2.8 and 3.2.9, the dynamic analysis results of the locomotive model have been shown on the same circular path. The lateral and vertical displacement values of the locomotive model decrease in comparison with the single wheelset's values because of the increased mass.

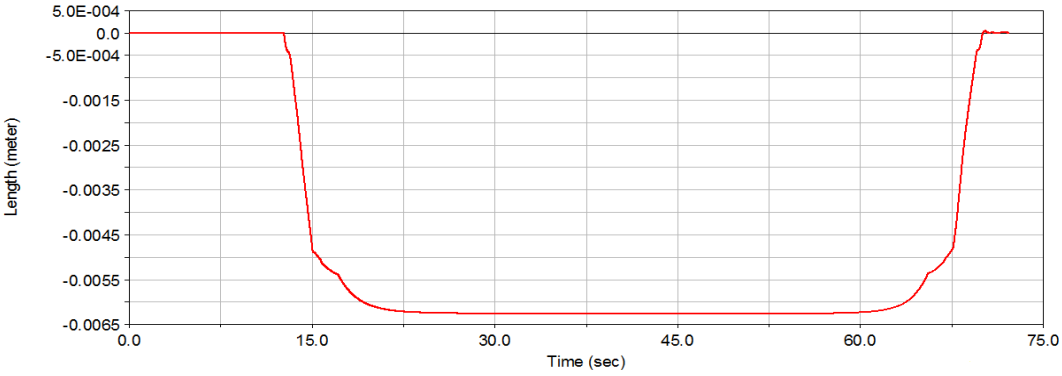

Figure 3.2.8. Lateral displacement of locomotive model on a circular path

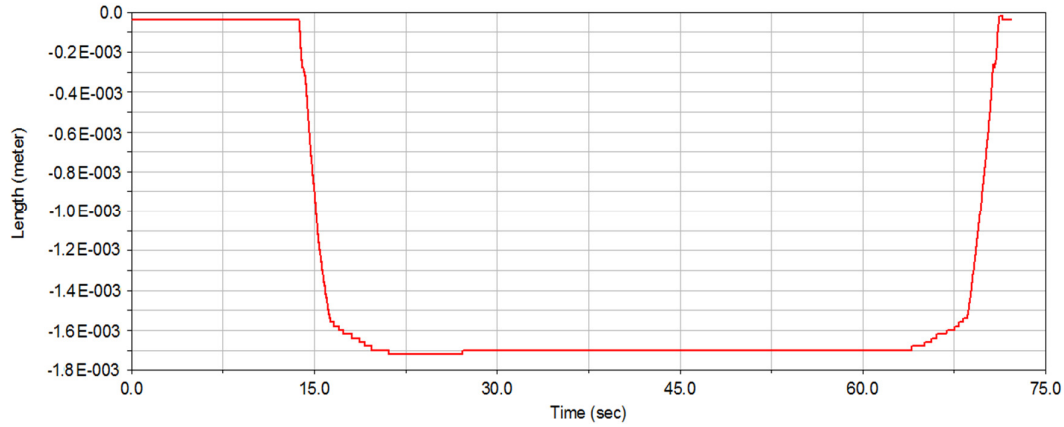

Figure 3.2.9. Vertical displacement of locomotive model on a circular path

4. CONCLUSION

This study focused on the continued development of the multibody system dynamics of rail vehicles. The development of the multibody dynamic model gives an opportunity to improve more realistic models. The modeling and simulation of rail vehicles are very important for high-speed trains in the way of safety, comfort and efficiency.

For this purpose, the significance of rail vehicle systems has been underlined in the thesis. It has been informed about the general circumstance of rail vehicle systems in the world and emphasized the importance of studies to be conducted in Turkey. Then, the general information about wheel-rail contact, rail vehicle systems, bogies and suspension systems has been presented and mentioned about their working principle. After introducing rail systems generally, the railway vehicle model similar to UM models of railway vehicles has been presented. A simplified model of locomotive E43000 has been described. The bodies in models have been created in ADAMS/Rail software with drawings, documentation and photos. The type of track irregularity has been chosen for this study with respect to the predefined standards. After the stability and dynamic analysis, the critical speeds, natural frequencies and the eigen values have been determined.

In the study, the first stability analysis has been made for a single wheelset model which has two degrees of freedom in lateral and rotational motion. The critical speed has been found as 16m/sec when the natural frequency is 0.55 Hertz and, this value shows similarity with the results generated with the equations of motion of wheelset. The second stability analysis is for bogie model with 22 degrees of freedom. The critical speed changes according to centre of gravity, moment of inertias and creep forces. The critical speed of bogie model has been found as 56 m/sec in 45 Hertz. The system is unstable and takes a risk of derailment. Then, the stability analysis of locomotive model which has about 70 degrees of freedom has been made on a straight way. The car body which assembled over three bogie subsytems has increased the critical speed from 56 m/sec to 67 m/sec. It means that, the systems become unstable in high speeds and take risks of derailment. Also, when the mass of rail vehicle increases, the critical speed of the systems increases, too.

In the dynamic analysis, the power spectrum density has been converted to irregularity randomly in terms of distance and phase angle using Fourier series in MATLAB. These studies have been made for six types of track irregularities and the second type of track irregularity has been approved for this study according to the data in TRENSIM project.

The dynamic analysis of experimental single wheelset, bogie and locomotive model on a straight track which occured in ADAMS/Rail have been represented in the second type of random track irregularity. The systems have performed a similar motion depending on the measured data of the systems in TRENSIM project. In both tests, the displacement values between -15 and +15 milimeter have been observed. Finally, the dynamic analysis of the single wheelset and locomotive model on a curved track have been made. In the analysis of single wheelset, a small displacement has been observed on the circular path. The lateral displacement value which is about 17 mm on the circular path shows similarity with the results which were generated with the equations of motion of wheelset. Also, it has been observed that, the lateral and vertical displacement values of the locomotive model decrease in comparison with the single wheelset's values because of the increased mass.

REFERENCES

[1] Kouroussis, G., Verlinden, O., Conti, C. (2010) Contribution of Vehicle/Track Dynamics to the Ground Vibrations Induced by the Brussels Tramvay. The 24th International Conference on Noise and Vibration Engineering, 20-22 September, Leuven, Vlaams Brabant, Belgium.

[2] Garg, V.K., Dukkipati, R.V. (1984) Dynamics of Railway Vehicle Systems, Academic Press, Toronto, Canada.

[3] Klingel, W. (1883) Uber den Lauf der Eisenbahnwagen auf Gerarder Bahn, Organ Fortsch. Eisenb, 38, 113-123

[4] Winans, R. (1829) British Patent 5796.

[5] Adams, W.B. (1863-1864) On the Impedimental Friction Between Wheel Tire and the Rails with Plans for Improvement, Proc. Instn. Civ. Engrs., 23, 411

[6] Redtenbacher, F. J. (1855) Die Gesetze des Locomotive-Baues, Verlag von Friedrich Bassermann, Mannheim, Stuttgart, Germany.

[7] Hertz, H. (1895) Gesamelte Werke, Leipzig, Germany.

[8] Carter, F.W. (1926) On the Action of Locomotive Driving Wheel. Proceedings of the Royal Society, Series A, Vol.112, 151-157.

[9] Markine, V. L. and Shevtsov, I. Y. (2011) Optimization of a Wheel Profile Accounting for Design Robustness, Proceedings of the Institution of Mechanical Engineers, Journal of Rail and Rapid Transit, 225-433.

[10] Shevtsov, I. Y. (2008) Wheel/rail Interface Optimisation, Technische Universiteit Delft, Holland.

[11] Jalili, M. M. and Salehi, H. (2011) Wheel/rail Contact Model for Rail Vehicle Dynamics, C. R. Mecanique 339, 700–707.

[12] Shen, G., Ayasse, J. B., Chollet, H., Pratt, I. (2003) A Unique Design Method for Wheel Profiles by Considering Contact Angle Function, Proceedings of the Institution of Mechanical Engineers, Part F: Journal of Rail and Rapid Transit, 217 (F3), 25-30.

[13] Iwnicki, S. D. And Evans, J. (2002) Vehicle Dynamics and Wheel/Rail Interface, Rail Technology Unit, Manchester Metropolitan University, Manchester, England.

[14] Agapov, D. (2008-2011) Description of Models of Locomotive E43000 and Train in Universal Mechanism Software, Bryansk State Technical University, Russia.

[15] Sperry, B. J. (2009) Complex Bogie Modeling Incorporating Advanced Friction Wedge Components, Masters of Science Thesis, Blacksburg, Virginia, ABD.

[16] Fujie, X., Jian, F., Lijian, G. Z. and Quanbao, F. (2011) Dynamic Analysis of the Electric Locomotive SS7CG with ADAMS/Rail, Zhu Zhou Electric Locomotive Institute, China.

[17] Müller, S., Kögel, R. and Schreiber, R. (2008) Simulation of a Locomotive as a Mechatronical System, ABB Corporate Research Center, Speyerer Str. 4, 69117 Heidelberg, Germany

[18] Michalek, T. and Zelenka, J. (2012) Dynamic Behaviour of Locomotive With Axle-Mounted Traction Motors. The 18th International Conference Engineering Mechanics, 2-14 May, Svratka, Czech Republic

[19] Harder, R. F. (2000) Dynamic Modeling and Simulation of Three-Piece North American Freight Vehicle Suspensions with Non-Linear Frictional Behaviour Using ADAMS/Rail. The 5th ADAMS/Rail User's Conference, 10-12 May, Haarlem, New York, USA

[20] Gugliotta, A and Soma, A (1996) Comparison of ADAMS/Rail Results With European Benchmark Data. The 11th European ADAMS User's Conference, November, Frankfurt, Germany

[21] Kalker, J. J. (1980) Review of Wheel Rail Contact Theories, Applied Mechanical Division Vol.40, ASME PP. 77-92

[22] Lee, S. Y. and Cheng, Y. C. (2008) A New Dynamic Model of High-Speed Railway Vehicle Moving on Curved Tracks, Journal of Vibration and Acoustics, February, Vol.130

[23] Ballew, B. S. (2008) Advanced Multibody Dynamics Modeling of the Freight Train Truck System, Masters of Science Thesis, Blacksburg, Virginia, ABD

[24] Zboinski, K. and Dusza, M. (2010) Extended Study of Railway Vehicle Lateral Stability in a Curved Track, Vehicle System Dynamics: International Journal of Vehicle Mechanics and Mobility, Vol. 49, No. 5, 789–810

[25] Uzzal, R. U. A., Ahmed, W. and Rakheja, S. (2008) Dynamic Analysis of Railway Vehicle-Track Interactions Due to Wheel Flat with a Pitch-Plane Vehicle Model, Department of Mechanical and Industrial Engineering Concordia University, Montreal, Canada

[26] Parena, D., Kuka, N., Vivalda, P. and Kik,W. (1988) Stability Investigations and Narrow Curving Analysis of a Streetcar Model, Fiat Ferroviaria, Savigliano (CN), Italy

[27] Shabana, A. A., Zaher, M. H., Recuero, A. M. and Rathod, C (2011) Study of Nonlinear System Stability Using Eigenvalue Analysis: Gyroscopic Motion, Journal of Sound and Vibration 330, 6006–6022

[28] Kar, A., Wormley, D.N. and Hedrick, J.K (1979). Performance Limits of Rail Passenger Vehicles: Evaluation and Optimization. Department of Mechanical Engineering, Massachusetts, ABD.

APPENDIX A. CREATING OF MODELS IN ADAMS/RAIL

This section presents how to create a locomotive model and its steps. The simulation software ADAMS/Rail specializes in the analysis of rail vehicles, as well as the different subsystems that constitute the model. These subsystems can be created by the user, using the creation mode templates, or it can use predefined templates for the program, facilitating the use of this software.

A.1. Creating a Bogie Template

It is necessary to create a template in which to build bogie parts. It should assign to the template a major role as a running gear template, because a major role defines the function the template serves for the vehicle.

To create a bogie template:

- From the file menu, select new.
- In the new template dialog box, enter “Bogie”, as template name.
- Verify that major role is set to running_gear.
- Verify that attachment type is set to single wagon attachment

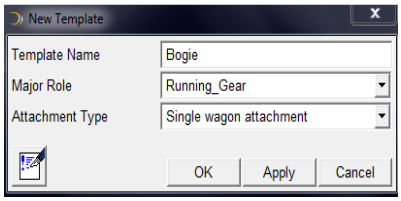

Figure A.1.1. New template dialog box

Then a gravity icon appears in the middle of the ADAMS/Rail main window as shown:

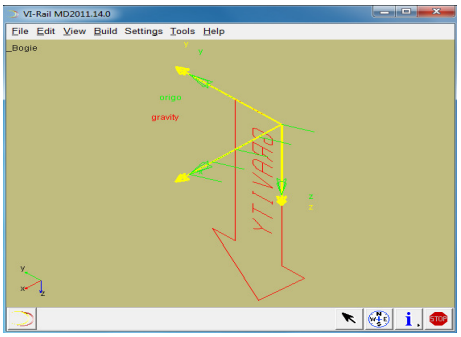

Figure A.1.2. Template builder

A.2. Creating Bogie Parts

In ADAMS/Rail, the general parts are created through a three-step process. First, you create hardpoints that define key locations on the part. Then, you create the actual part. Finally, you add geometry to your new part if necessary.

A.2.1. Creating the wheelsets

First the wheelsets and a hardpoint are defined. Later, this hardpoint is modified to determine its effect on the vehicle. Next, a double wheelset is created and specified its coordinate system location, the wheels' property files, and mass properties.

To build the hardpoint:

- From the build menu, point to hardpoint, and then select new.
- In the create hardpoint dialog box, enter reference as hardpoint's name.
- Verify that type is set to single.
- Specify the location

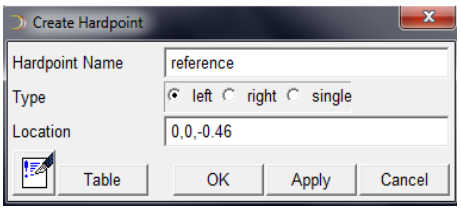

Figure A.2.1. Hardpoint dialog box

To create the wheelsets: From the build menu, point to railway elements, point to wheelset, point to double wheelset,and then select new.

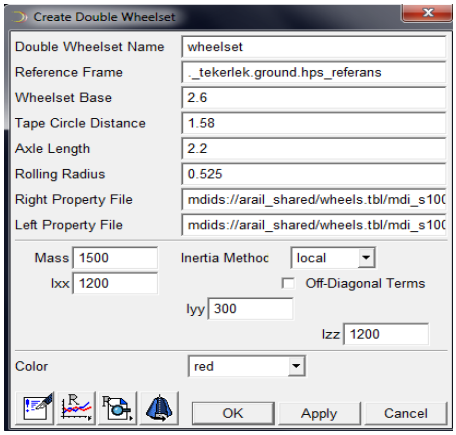

Figure A.2.2. Wheelset dialog box

VI-Rail creates a double wheelset component, where each wheelset has the specified mass properties. To see the double wheelset in the main window, fit the model to view.

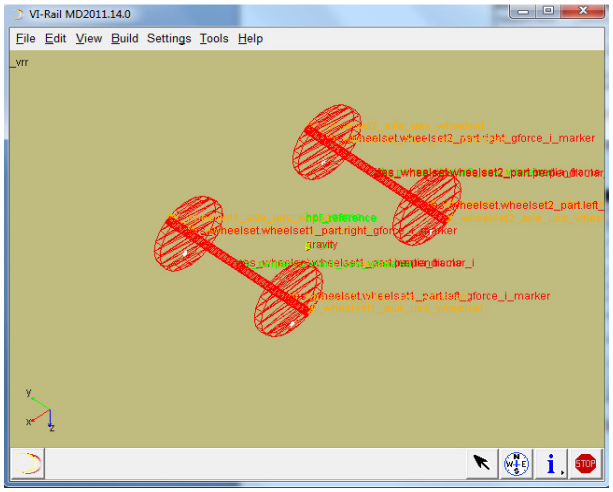

Figure A.2.3. Double wheelset

A.2.2. Creating the bogie frame

To create the bogie frame:

- From the build menu, point to railway elements, point to bogie frame, and then select new.
- Fill in the dialog box as shown next, and then select OK.

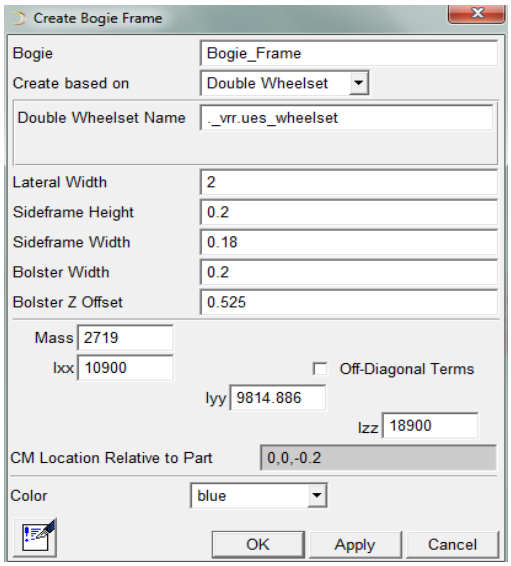

Figure A.2.4. Bogie frame dialog box

The template looks as shown next:

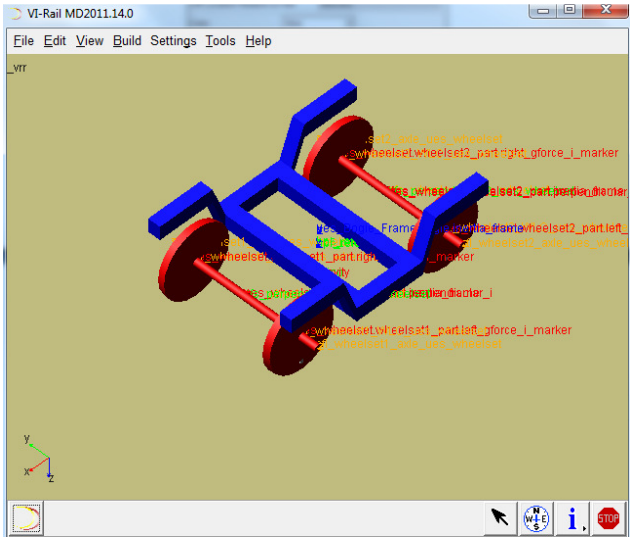

Figure A.2.5. Bogie frame design

A.2.3. Creating the axle-boxes

To create the two front axle boxes:

- From the build menu, point to railway elements, point to axle box, and then select new.
- Fill in the dialog box as shown next, and then select OK.

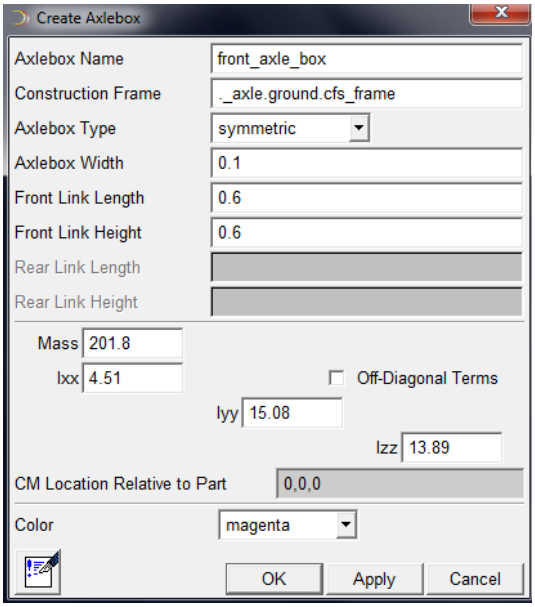

Figure A.2.6. Axle-box dialog Box

Then to create the rear axle boxes, you modify the dialog box entries, construction frame and center of mass of location relative to the part. The template looks as shown next:

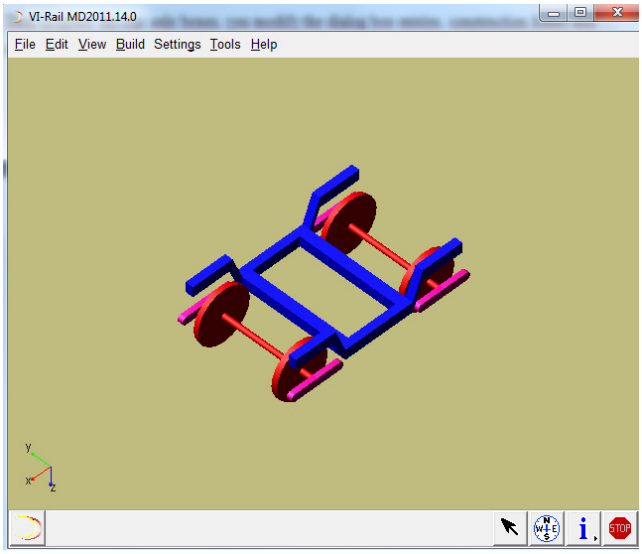

Figure A.2.7. Axle-box design

A.2.4. Creating the primary suspensions

To create the primary suspensions:

- First, the construction frames are created and used to define the suspensions.
- From the build menu, point to construction frame, and then select new.
- Fill in the dialog box as shown next and select apply.

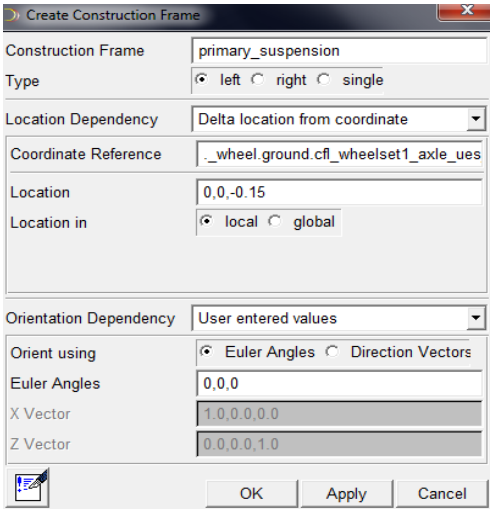

Figure A.2.8. Construction frame dialog box

To build the suspensions:

- From the build menu, point to suspension element, and then select new.
- Fill in the dialog box as shown next, and then select OK.

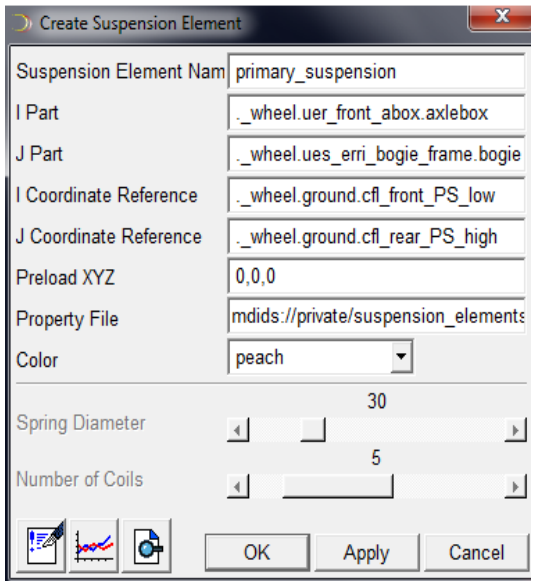

Figure A.2.9. Suspension element dialog box

The template looks as shown next:

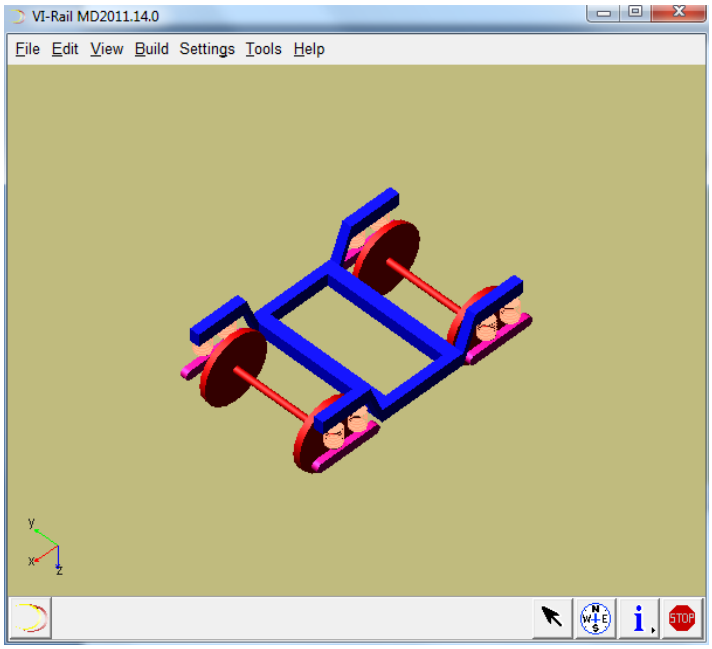

Figure A.2.10. Primary suspension design

A.2.5. Creating the secondary suspensions

Before creating the secondary suspensions for the bogie, you must first create the mount part which connects to the wagon part during assembly. A mount part is a massless part, fixed to the ground by default. This part represents the wagon part and acts as a place holder for it.

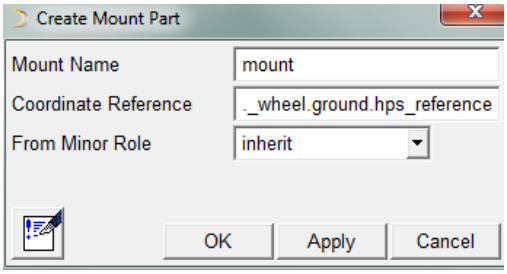

Figure A.2.11. Mount part dialog box

To create the secondary suspensions:

- From the build menu, point to construction frame, and then select new.
- Fill in the dialog box and select apply.
- Create the other construction frame with specifying location.
- Finally create the two secondary suspensions as shown next.

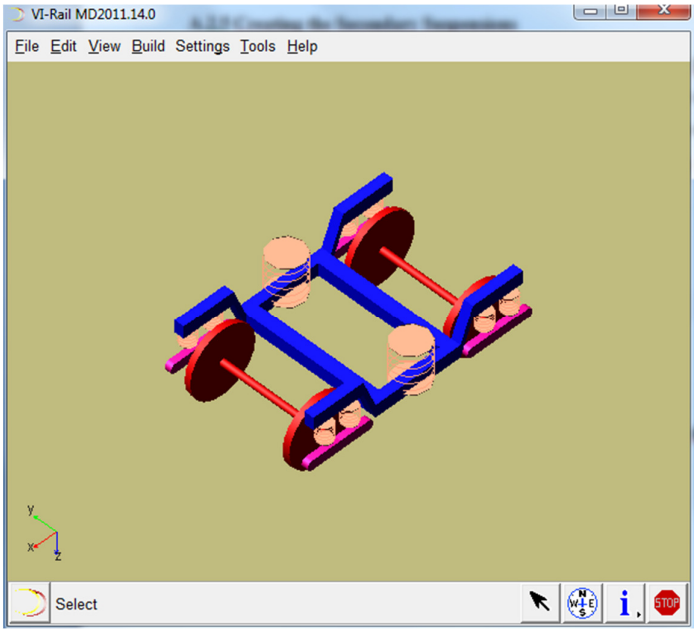

Figure A.2.12. Secondary suspension design

A.2.6. Creating the vertical, lateral and anti-yaw dampers

First, the hardpoints are created and used along with the property file that is provided to define the damper. Property files define characteristics for springs, dampers, bumstops and bushings.

To define a damper, the following must specified:

- Two bodies between which wanted to force to act.
- Specific location on each body where the force acts.
- Series stiffness.
- Property file, which contains the damper's force-velocity curve.

The damping type can be:

- Linear damping
- Linear damping + series stiffness
- Nonlinear damping
- Nonlinear damping + series stiffness

To create the secondary dampers:

- Fill in the dialog boxes for vertical, lateral and anti-yaw dampers as shown next
- Select apply

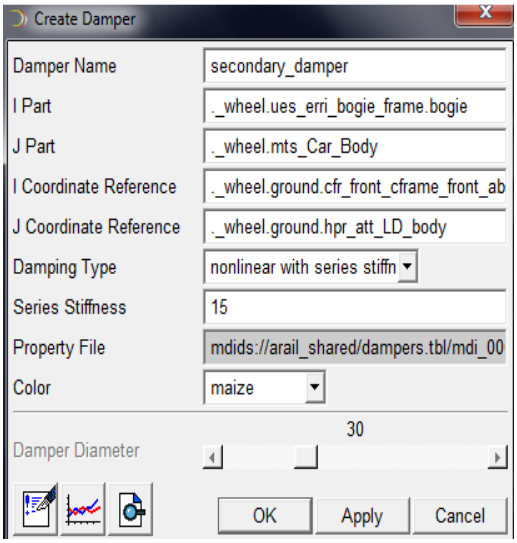

Figure A.2.13. Secondary dampers dialog box

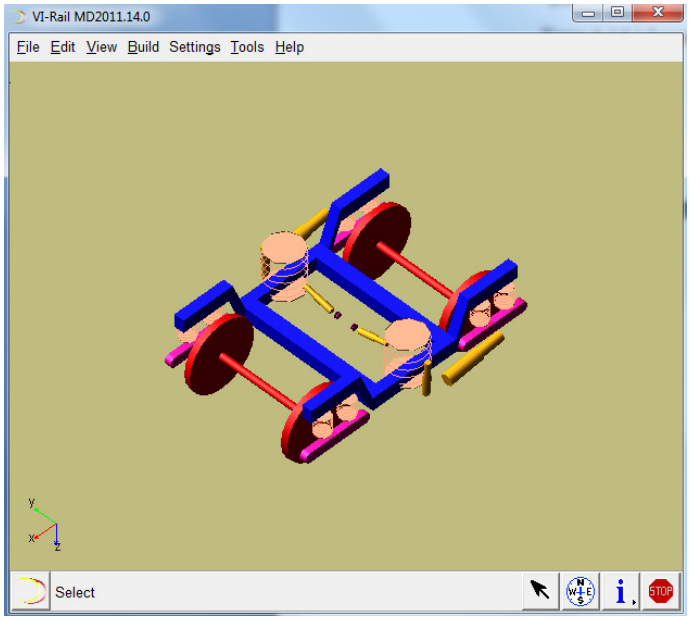

Figure A.2.14. Secondary dampers design

A.2.7. Creating the wheelset electromotor block (WEB) subsystem

In ADAMS/Rail model, the mass of each wheelset electromotor block subsystem has been reduced to the mass of bogie frame.

To create the WEB subsystem:

- First, the cylinder geometry is created and used to define the WEB subsystem.
- From the build menu, point to cylinder geometry, and then select new.
- Fill in the dialog box as shown next and select apply.

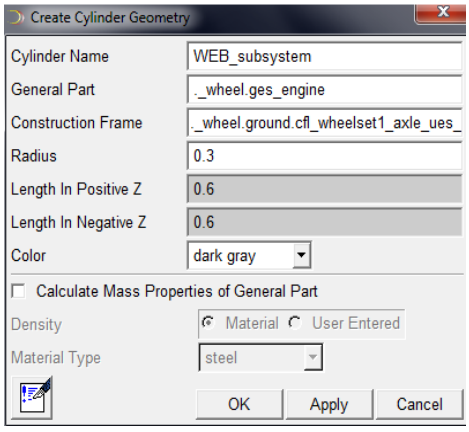

Figure A.2.15. WEB subsystem dialog box

Finally, the bogie model looks as shown next:

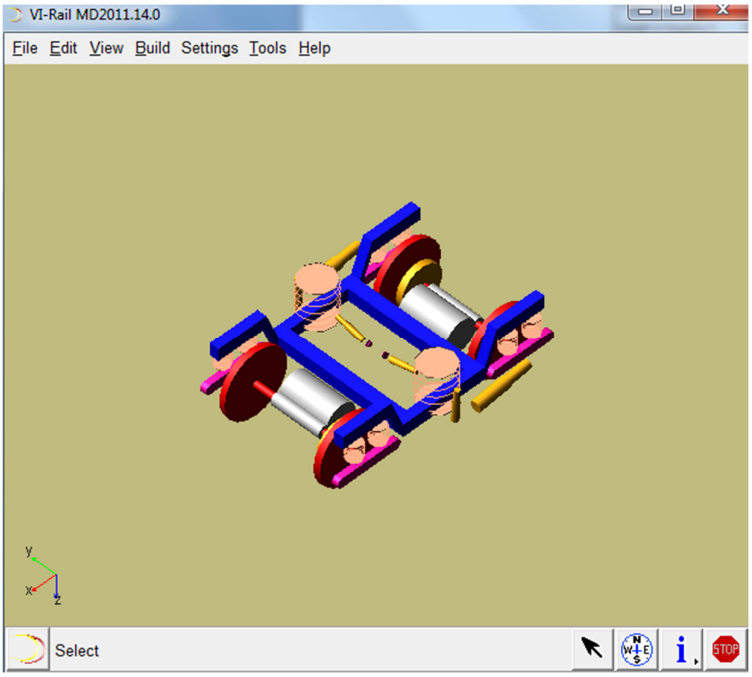

Figure A.2.16. Bogie model

A.3. Creating a Car Body Template

In this section, a template is created for the wagon part. A car body is assigned as the major role fort he template. A major role defines to function the template serves for the vehicle.

Before creating the wagon part, a hardpoint is created for it.

To create a template:

- Create a template named as “body”.
- Verify that major role is set to car body.
- Select OK.

ADAMS/Rail displays a gravity icon.

To build the hardpoint:

- Create a hardpoint with necessary specifications
- Specify the location
- Choose single type

To create the wagon part:

- From the build menu, point to railway elements, point to car body, point to passenger wagon, and then select new.
- Fill in the dialog box as shown next, and then select OK.

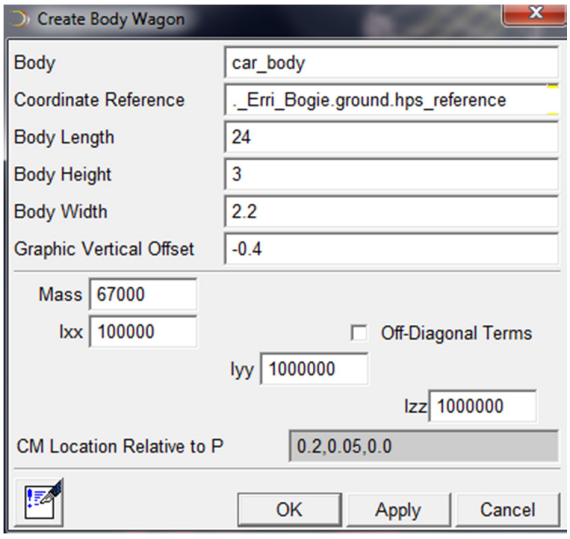

Figure A.3.1. Body wagon dialog box

The following shows a right side view of the template:

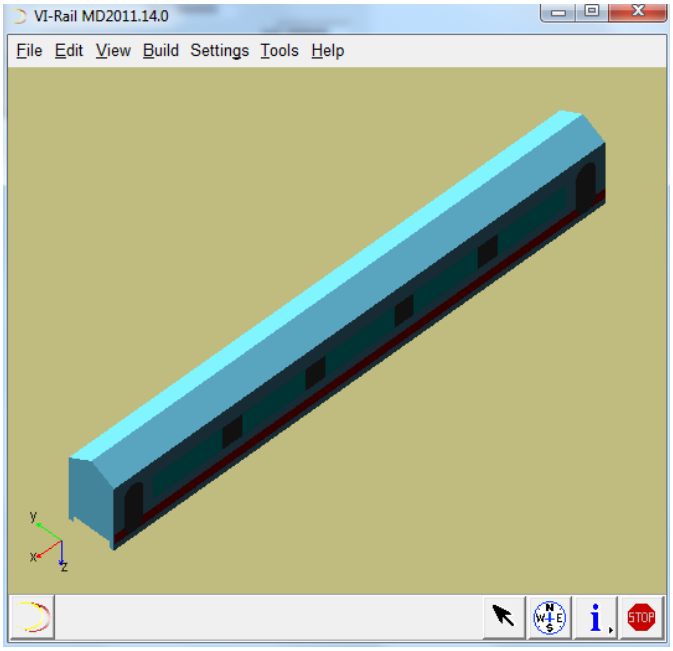

Figure A.3.2. Body Wagon

A.4. Creating a Full Rail-Vehicle Assembly

In this section, full rail-vehicle assembly is created. Using ADAMS/Rail, it can be grouped separate subsystems into an assembly. A full rail-vehicle assembly contains front, rear and middle bogies and a car body.

To create a full rail-vehicle assembly:

- From the file menu, point to new, and then select wagon assembly.
- In the assembly name text box, enter Wagon in the new wagon assembly dialog box.
- Select the folder icon next to body subsystem.
- Right-click the other subsystems text box, point to search, and then select the private database and select open as shown next.

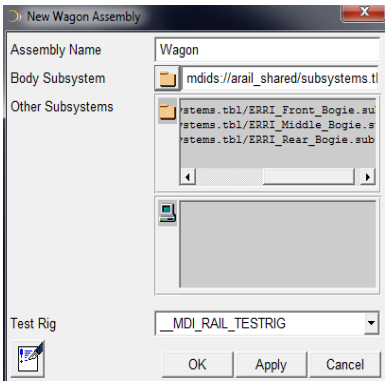

Figure A.4.1. Wagon assembly dialog box

Finally, ADAMS/Rail displays the full assembly in the main window, as shown next:

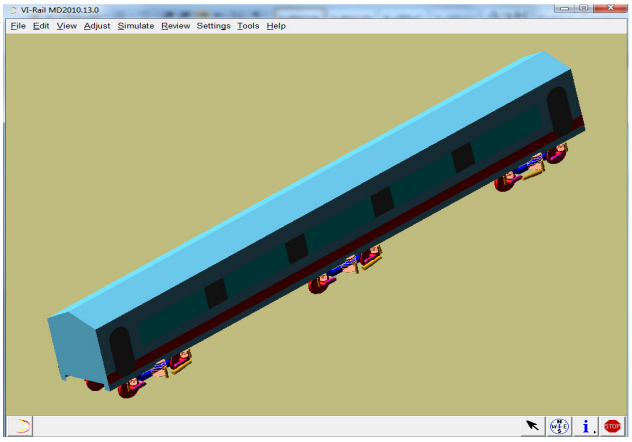

Figure A.4.2. Full rail vehicle assembly

APPENDIX B. TYPES OF TRACK IRREGULARITIES

This section presents the different types of track irregularities introduced in Chapter 2.1.

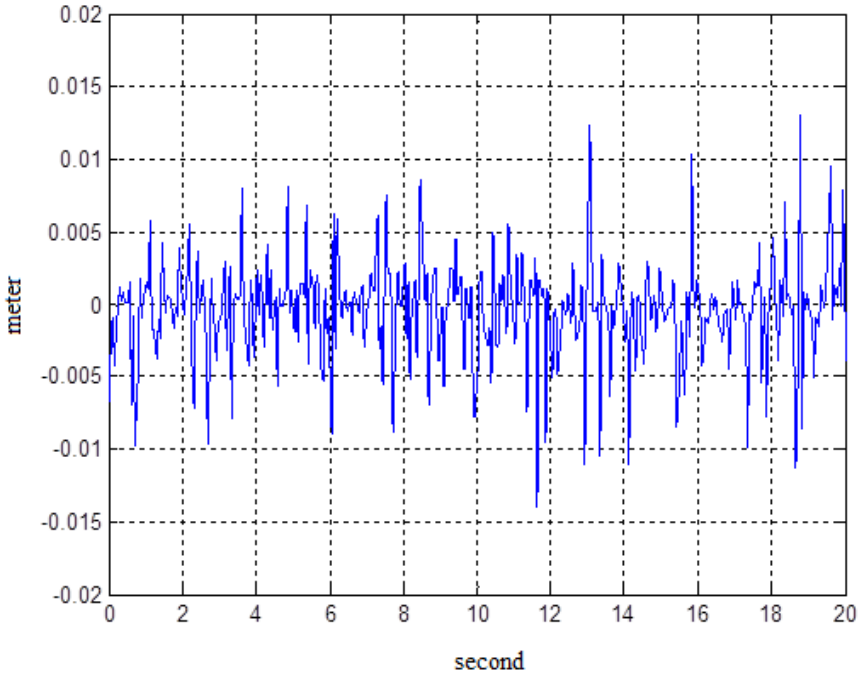

Figure B.1. First type of track irregularity [1]

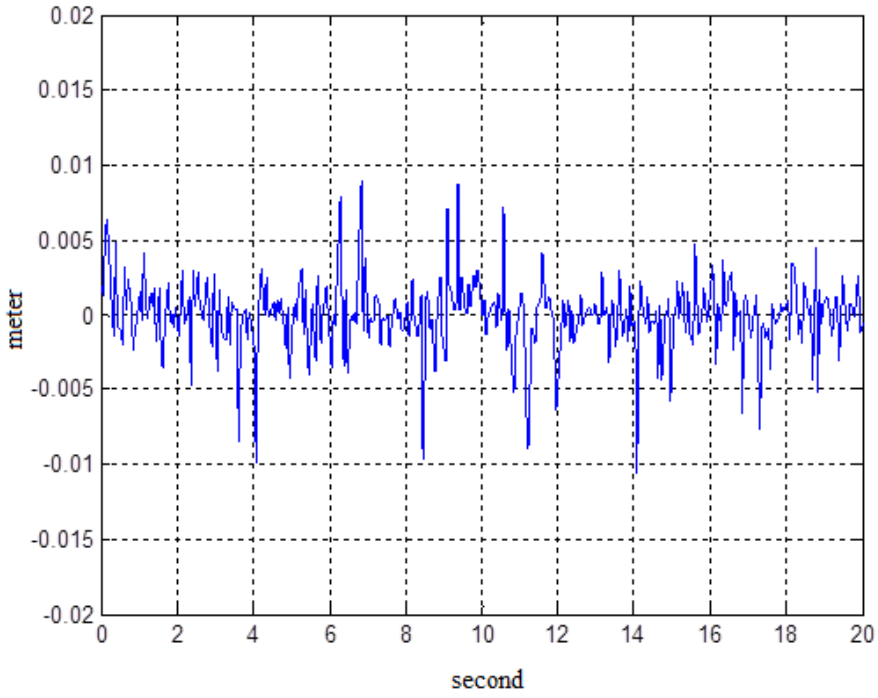

Figure B.2. Second type of track irregularity [1]

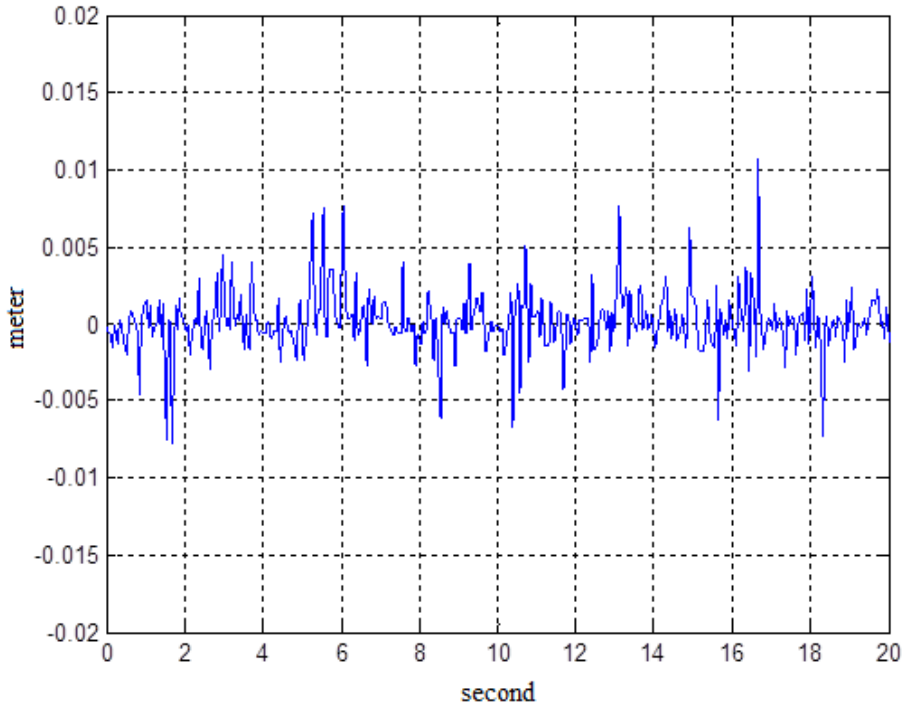

Figure B.3. Third type of track irregularity [1]

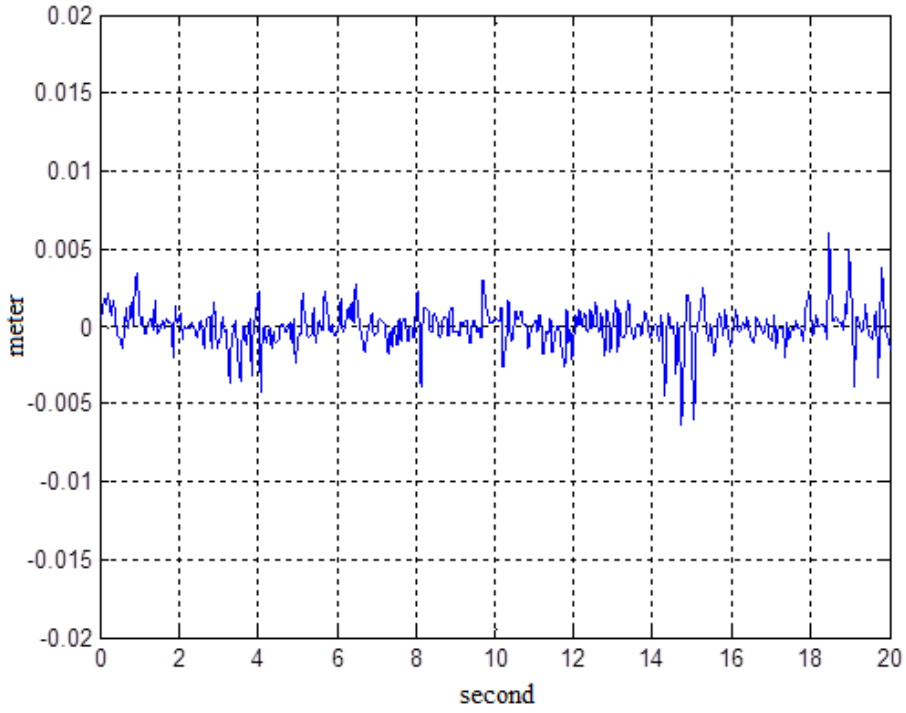

Figure B.4. Fourth type of track irregularity [1]

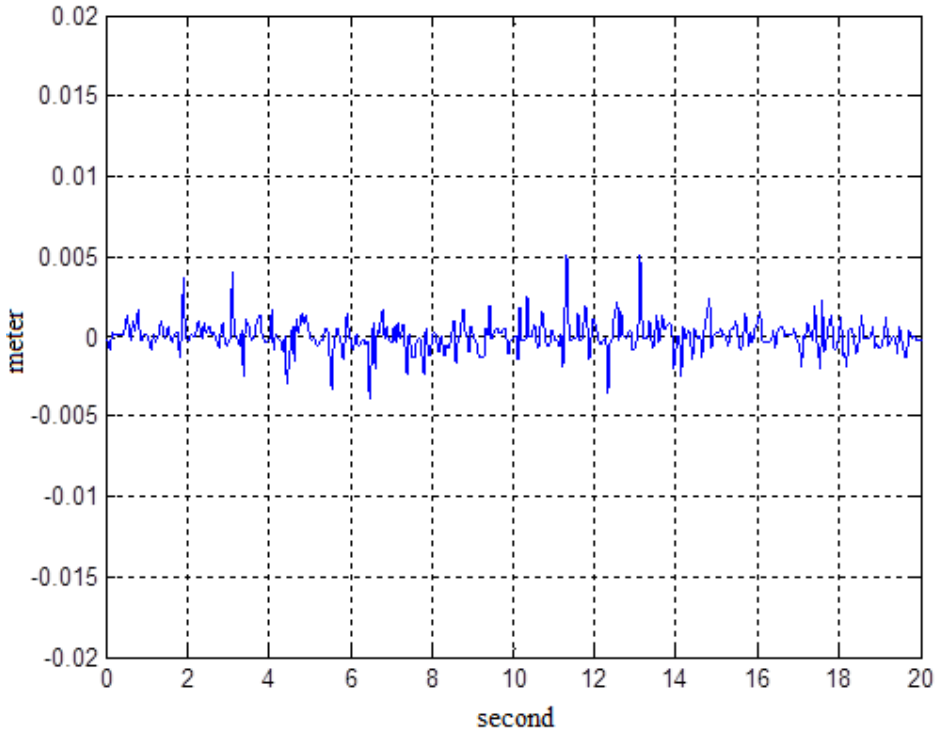

Figure B.5. Fifth type of track irregularity [1]

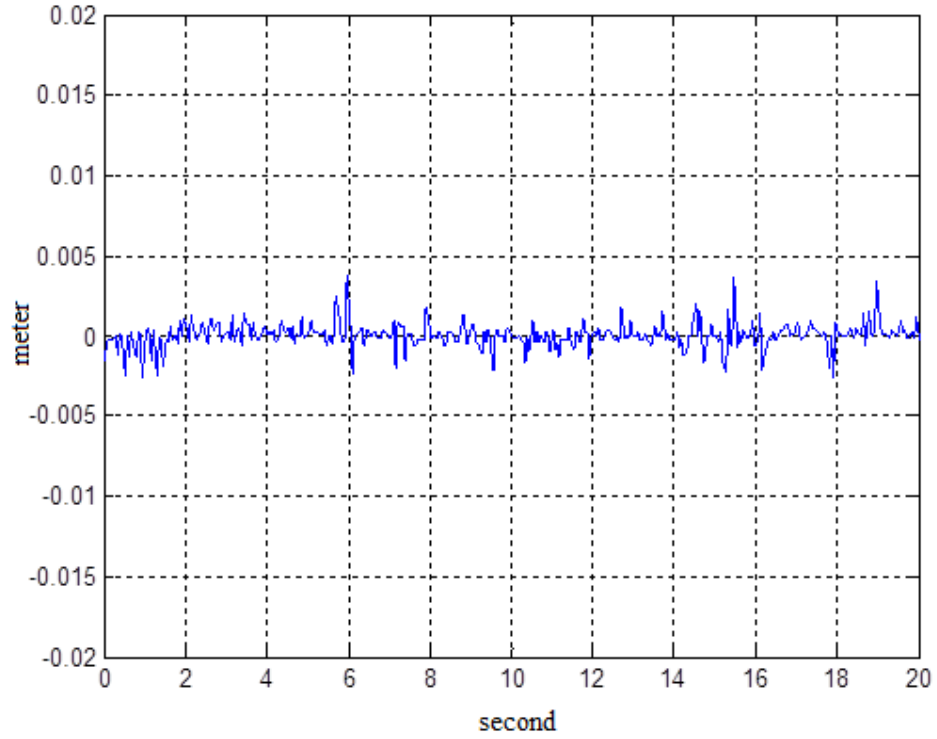

Figure B.6. Sixth type of track irregularity [1]

APPENDIX C. EQUATIONS OF MOTION OF SINGLE WHEELSET

This section presents the equation derivation for the single wheelset which has two degrees of freedom. Applying Newton's Law in the lateral (y) and yaw (Ψ) direction, the model is shown in figure C.1, which is the same model introduced in Chapter 2.2.3.

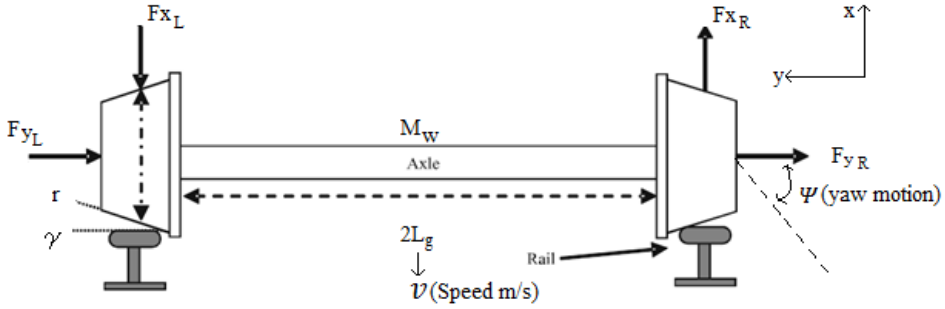

Figure C.1. Free body diagram of single wheelset

$$M_w\ddot{y} = -F_{yR} - F_{yL}$$

$$I_w\ddot{\Psi} = F_{xR}L_g - F_{xL}L_g \quad \text{(C.1)}$$

and,

$$F_{yL} = F_{yR} = f_{11}.\xi_y + f_{12}.\xi_{SP}$$

$$F_{xL} = -F_{xR} = f_{33}.\xi_x \quad \text{(C.2)}$$

where

f_{11}, f_{12}, f_{33} = creep coefficients and ξ_x, ξ_y, ξ_{SP} = creepages

also,

$$\xi_x = \frac{\gamma}{r_o}.y + \frac{L_g}{v}.\dot{\Psi}$$

$$\xi_y = \frac{\dot{y}}{v} - \Psi$$

$$\xi_{SP} = \frac{\dot{\psi}}{v} \quad \text{(C.3)}$$

Finally, we have two general equations for a single wheelset:

$$M_w.\ddot{y} = -2f_{11}\left(\frac{\dot{y}}{v} - \Psi\right) - 2f_{12}.\frac{\dot{\Psi}}{v}$$

$$I_w.\ddot{\Psi} = -2f_{33}\left(\frac{L_g.\gamma.y}{r_0} + \frac{{L_g}^2.\dot{\Psi}}{v}\right) \quad \text{(C.4)}$$

On a curved track, the model can thus be described by the following equations:

$$M_w.\ddot{y} = -2f_{11}\left(\frac{\dot{y}}{v} - \Psi\right) - 2f_{12}.\frac{\Psi}{v} + m_w.\left(\frac{{v_s}^2}{R} - g\theta_c\right)$$

$$I_w.\ddot{\Psi} = -2f_{33}\left(\frac{L_g.\gamma.y}{r_0} + \frac{{L_g}^2.\dot{\Psi}}{v} + \frac{{L_g}^2}{R}\right) \quad \text{(C.5)}$$

where

R is radius of curvature and θ_c is cant angle.

When we assume that the single wheelset realizes a steady-state motion on a curved track the lateral displacement of the pure rolling line from the track centre-line may be written as:

$$y = \frac{r_0.L_g}{R.\gamma} \quad \text{(C.6)}$$

where

$r_0 = 0.525$ m

$L_g = 1.58$ m

R = 300 m

$\gamma = 0.2$ rad